

## SunQM-4s2: Using {N,n} QM and non-Born probability to analyze Earth atmosphere's global pattern and the local weather

Yi Cao

e-mail: yicaojob@yahoo.com

© All rights reserved. Submitted to viXra.org on 7/1/2020.

### Abstract

In this paper, we tried to use the non-Born probability (NBP, developed in SunQM-4) to describe Earth atmosphere's phenomenon in  $\theta\phi$ -2D dimension. After analyzing Earth atmosphere's global circulation pattern, we found that it is related only to the  $\theta$ -1D QM. Because the spinning Earth's  $\theta$ -1D dimensional matter wave is in a true standing wave mode, we found that the Born probability analysis gives more sharp and conclusive result than that of the NBP analysis. Earth atmosphere's elliptical shape is caused by that the  $|2,1,1\rangle$  QM state is the most heavily populated (by air mass); its Hadley/Ferrel/Polar global circulation cells are formed by the  $|2,1,1\rangle$  QM's mass-peaking effect at  $0^\circ$  latitude and  $|2,1,0\rangle$  QM's mass-peaking effect at  $60^\circ$  latitude; and its jet streams may can be explained as the residue  $|3,2,1\rangle$  and  $|3,2,0\rangle$  states embedded in the extremely suppressed  $|2,0,0\rangle$  sub-shell. To describe Earth's local weather, we have to use NBP because it gives  $\phi$  (besides  $\theta$ ) dimensional information. We demonstrated that a hurricane's low air pressure center can be described by a NBP density minimum center (or a negative peak of a combined  $\text{Re}[Y(l,m)]$  wave functions); an hurricane array can be described by that a single wave function mode of  $\text{Re}[Y(l,m)]$  is (unevenly) amplified; the polar vortex's low air pressure center can be described by a NBP density minimum center (or a negative peak of a combined  $\text{Re}[Y(l,m)]$  wave functions) of low temperature; a single day (7/22/2018)'s extreme weather can be described by that a single wave function mode of  $\text{Re}[Y(l=9,m=7)]$  was (unevenly) amplified; El Nino related warm/cold water pools oscillation can also be explained by NBP in a combined  $\text{Re}[Y(l,m)]$ , or by the 1D infinitely deep potential well QM. This work clearly revealed the true physical meaning of the QM's wave function: it is the probability density of a physical variable's value, although in the wave form. Also, the physical meaning of the Schrodinger equation becomes: it directly describes a dynamic distribution of a physical variable's value (although in its probability's wave form).

### Introduction

The SunQM series research articles <sup>[1]-[16]</sup> have demonstrated that the formation of Solar system (as well as each planet) was governed by its {N,n} QM. In SunQM-4 <sup>[17]</sup>, we showed that the non-Born probability (NBP) is needed for the full-QM deduction of Solar system's 3D probability density map with orbital movement. In SunQM-4s1 <sup>[18]</sup>, we showed that the NBP is a valid not only for {N,n} QM, but also for the 1D infinite deep square potential well QM (1D $\infty$ QM), for the circular 1D QM, and for the plane wave QM. Furthermore, with NBP, we can explain the flute sound wave (an air mass density vibration) mechanics directly as the 1D $\infty$ QM! This leads us to further explore Earth's atmosphere (wave) pattern by using NBP (in the current paper) because it is also related to air mass density vibration. QM theory had been used to explain Earth atmosphere's global circulation pattern in SunQM-3s3 <sup>[9]</sup>. Recently, we see some other scientists also start to use QM to explain Earth's extreme weather <sup>[19]</sup>. In the current paper, we (as citizen scientist) try to throw all atmospheric and weather phenomena into the box of {N,n} QM, and shake the box around to push everything to fit in (even some are not perfectly fitted in). Note: for {N,n} QM nomenclature as well as the general notes for {N,n} QM model, please see SunQM-1 section VII. Note: Microsoft Excel's number format is often used in this paper, for example:  $x^2 = x^2$ ,  $3.4E+12 = 3.4 \times 10^{12}$ ,  $5.6E-9 = 5.6 \times 10^{-9}$ . Note: The reading sequence for SunQM series papers is: SunQM-1, 1s1, 1s2, 1s3, 2, 3, 3s1, 3s2, 3s6, 3s7, 3s8, 3s3, 3s9, 3s4, 3s10, 3s11, 4, 4s1 and 4s2. Note: for all SunQM series papers, reader should check "SunQM-4s7: Updates and Q/A for SunQM series papers" for the most recent updates and corrections.

## I. Using $\theta$ -dimensional Born probability or NBP to explain Earth atmosphere's global circulation pattern

### I-a. Spinning $\{N,n\}$ QM's nLL effect re-shapes Earth atmosphere from a spherical shape to an elliptical shape

As mentioned in SunQM-3s3, let's first define Earth has a  $p\{N,n//2\}$  QM structure, with Earth's inner core has the size of  $p\{0,1//2\}$ . Then Earth's outer core plus mantles is in  $p\{0,1//2\}$  QM orbital shell space, or in  $|n,l,m\rangle = |1,0,0\rangle$  QM state (see Figure 1a). Hence Earth's atmosphere must be in  $p\{1,1//2\}$  or  $p\{0,2//2\}$  QM orbital shell space (see Figure 1a), or in  $|n,l,m\rangle = |2,l,m\rangle$  QM state, where  $l = 0, 1$ , and  $m = -l \dots +l$ , that is,  $|2,0,0\rangle$ ,  $|2,1,0\rangle$ ,  $|2,1,1\rangle$ , and  $|2,1,-1\rangle$ . These four QM states can be further divided into two spherical  $l$  sub-shells: the inner  $l=1$  spherical sub-shell is made of the combination of three QM states  $|2,1,0\rangle$ ,  $|2,1,1\rangle$ , and  $|2,1,-1\rangle$ , and the outer  $l=0$  spherical sub-shell is made of  $|2,0,0\rangle$  QM state alone. If the Earth does not self-spin, then all these four QM states have the same QM state energy, so these four QM states are degenerated (meaning hybridized, or indistinguishable), and the atmospheric air mass will distribute evenly among these four QM states, therefore atmosphere will form a perfect sphere shape. After Earth self-spinning, and after defining that  $m = +l$  correlates to the Earth spin direction, then  $|2,1,-1\rangle$  QM state is no longer available for Earth's atmosphere (because it means that the Earth's atmosphere moves in the opposite direction to Earth's spin). According to the gravity force caused nLL QM effect (see SunQM-3s1 and SunQM-3s3), a spinning Earth's  $p\{0,2//2\}$  QM will differentiate the QM state energy for each of four  $|2,l,m\rangle$  QM states, so that  $|2,1,1\rangle$  has the lowest state energy,  $|2,1,0\rangle$  has a higher state energy, and  $|2,0,0\rangle$  has the highest state energy. Therefore, air mass is re-distributed with more in the  $|2,1,1\rangle$  QM state, less in  $|2,1,0\rangle$  QM state, and most zero in  $|2,0,0\rangle$  QM state, therefore Earth atmosphere becomes a M&M candy shape (as shown in Figure 1d or Figure 1g). In the modeling using Born probability (see Figure 1e through Figure 1g), if we add  $1/3$  of air mass in  $|Y(1,0)|^2$ ,  $1/3$  of air mass in  $|Y(1,1)|^2$ , and  $1/3$  of air mass in  $|Y(1,-1)|^2$ , it will generate  $l=1$  sub-shell as a perfect sphere (correlates to the non-spin Earth, figure not shown). However, if we add  $1/5$  of air mass in  $|Y(1,0)|^2$ , and  $4/5$  of air mass in  $|Y(1,\pm 1)|^2$ , it ends as a M&M candy shaped  $l=1$  sub-shell as shown in Figure 1g (to roughly mimic Figure 1d's shape).

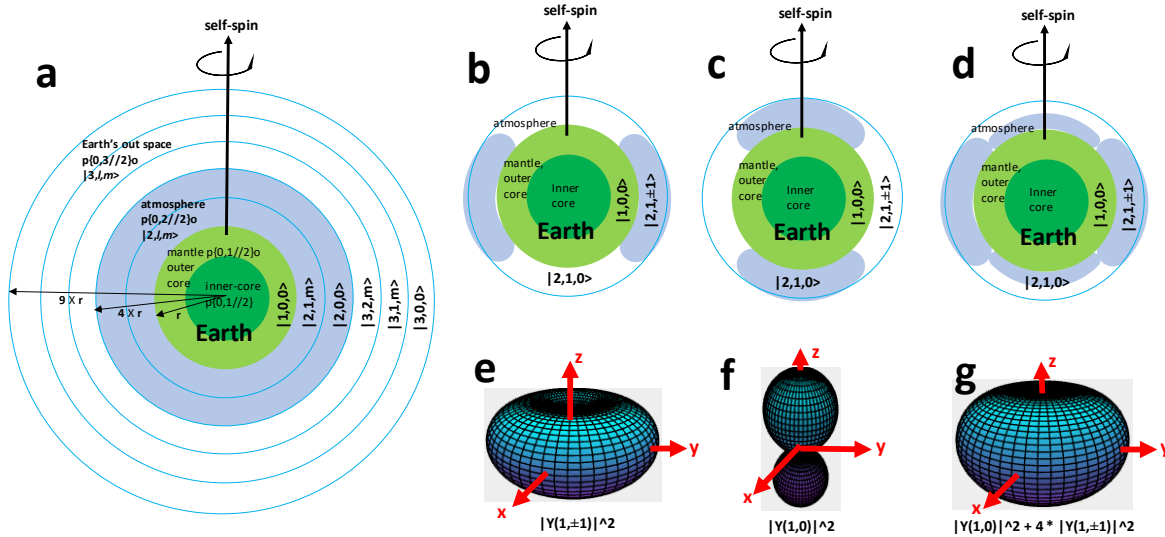


Figure 1a. Illustration of the  $\{N,n//2\}$  QM structure of Earth's atmosphere (including Earth's inside and Earth's out-space).

Notice that the thickness of each  $n$  shell (or each  $l$  sub-shell) is drawn in an arbitrary scale (for Figures 1a through 1d).

Figure 1b. Illustration of the atmospheric air mass (see light blue color) is purely in  $|2,1,1\rangle$  QM state.

Figure 1c. Illustration of the atmospheric air mass (see light blue color) is purely in  $|2,1,0\rangle$  QM state.

Figure 1d. Illustration of the atmospheric air mass (see light blue color) is mostly in  $|2,1,1\rangle$  QM state, and small amount in  $|2,1,0\rangle$  QM state.

Figures 1e. Spherical 3D plot of the Born probability  $|Y(1,\pm 1)|^2$ , using MathStudio (<http://mathstud.io/>) software.

Figures 1f. Spherical 3D plot of the Born probability  $|Y(1,0)|^2$ .

Figures 1g. Spherical 3D plot of  $|Y(1,0)|^2 + 4 * |Y(1,\pm 1)|^2$ , try to illustrate the air mass distribution in Figure 1d.

Notice that in Figure 1a, the thickness of each  $n$  shell (or each  $l$  sub-shell) is drawn in an arbitrary scale. The total  $n=2$  shell thickness should be from  $r = 4 * r_1$  ( $= r_{\text{Earth}}$ , because  $r_1 = r_{\text{Earth}}/4$ ) to  $r = 9 * r_1$  ( $= 9 * r_{\text{Earth}}/4$ ). The total  $n=3$  shell thickness should be from  $r = 9 * r_{\text{Earth}}/4$  to  $r = 16 * r_{\text{Earth}}/4$ . However, Earth's atmosphere has too little air mass to fully occupy the whole  $|2,l,m\rangle$  shell space, or even for the  $|2,l=1,m\rangle$  sub-shell space. According to wiki "atmosphere of Earth" Figure "Comparison of the 1962 US Standard Atmosphere graph of geometric altitude against air density, pressure", Earth atmosphere's air mass density at the top end of troposphere ( $\sim 12$  km high) is  $\sim 25\%$  of that at the sea level, and at 20 km altitude is only  $\sim 7\%$ . Then we can reasonably assume that the effective thickness of the  $n=2$  shell for the air mass is greatly suppressed to  $\sim 12$  km thick (i.e., from sea level to  $\sim 12$  km above), in comparison to the original from  $r/r_1 = 4$  (or the sea level) through  $r/r_1 = 9$  (or  $= 9/4 * r_{\text{Earth}} - r_{\text{Earth}} = (9/4 - 1) * 6.38E+3 = 7975$  km above the sea level). According to my (citizen level scientific) guess, for most part of the air mass, the troposphere ( $0 \sim 10$  km) can be counted as  $|2,l=1,m\rangle$  sub-shell, and the tropopause ( $10 \sim 12$  km) can be counted as  $|2,l=0,m=0\rangle$  sub-shell (see Figure 3 for more explanation).

### I-b. Spinning $\{N,n\}$ QM's mass-peaking and mass-depleting effect formed Earth atmosphere's Hadley/Ferrel/Polar global circulation cells

Section I-a described an elliptical shaped Earth atmosphere, spinning with Earth's spin, and no lateral air flow (therefore no weather). In SunQM-3s3 section III, we had showed that we can also use Schrodinger equation's solution ( $\Psi_{nlm} = R_{nl} * Y_{lm}$ ) and Born probability ( $r^2 * |\Psi_{nlm}|^2 = r^2 * |R_{nl}|^2 * |Y_{lm}|^2$ ) to explain Earth atmosphere's global circulation pattern with Hadley/Ferrel/Polar global circulation cells. As shown in Table 1 (columns 7 ~ 9) and Figure 2a,  $|2,1,1\rangle$  QM state's Born probability in  $\theta$ -2D dimension  $|Y(1,1)|^2$  peaks at  $\theta = \pi/2$  (or at equator), therefore (we explained it as that) it is  $|2,1,1\rangle$  QM state's mass-peaking force at  $\theta = \pi/2$  causes the air mass up-welling at the Earth's equator. Similarly,  $|2,1,0\rangle$  QM state's Born probability  $|Y(1,0)|^2$  peaks at  $60^\circ$  latitude (after corrected the  $\theta'$  to  $\theta' * 0.9$  for the centrifugal force, see SunQM-3s3 for details), therefore (we explained it as that) it is  $|2,1,0\rangle$  QM state's mass-peaking force at  $\theta' = \pm 60^\circ$  causes the air mass up-welling at the Earth's  $60^\circ$  latitude. In between equator and  $60^\circ$ , the QM mass-depleting force at Earth's  $30^\circ$  latitude causes the air mass down-welling there.

With the new concept of non-Born probability (NBP, developed in SunQM-4 and SunQM-4s1), now we can explain the same Hadley/Ferrel/Polar cells by using NBP. The NBP calculation (shown in columns 10 through 13 of Table 1) so far is still a citizen scientist leveled calculation (meaning based only on the scientific guess, not on the strict math deduction). To make it work, first, we need to expand NBP concept from  $nLL$  QM state to all  $|n,l,m\rangle$  QM states. Then we need to figure out what is the NBP formula for the non  $nLL$  states. At this time, we still don't know how to work it out exactly. So in columns 10 through 13 of Table 1 (for Figure 2d), we simply: a) changed  $\sin(\theta) \rightarrow [1 + \sin(\theta)]/2$ , and  $\cos(\theta) \rightarrow [1 + \cos(\theta)]/2$ ; b) for the  $\theta$ -dimensional wave of  $Y(1,0)$ , used  $\theta$  as the forward wave (represented as +NBP in the Table or the figure), and used  $\pi - \theta$  as the backward wave (represented as -NBP in the table or the figure), and present them separately as shown in Figure 2d (forward wave as the dash-line, backward wave as the dot-line); c) for the  $\theta$ -dimensional wave of  $Y(1,1)$ , only calculate  $\varphi=0$  position so that  $Y(1,1) = -1/2 * \sqrt{3/2\pi} * \exp(i * \varphi) * \sin(\theta) = -1/2 * \sqrt{3/2\pi} * \sin(\theta)$ , and the forward wave plus the backward wave equals to  $Y(1,1)$  after normalization, and remove the negative sign (for probability  $\geq 0$ ), so that  $Y(1,1,NBP) * \sin(\theta) = 1/2 * \sqrt{3/2\pi} * [(1 + \sin(\theta))/2 * \sin(\theta)]$ . Note: the last  $* \sin(\theta)$  comes from the spherical integration  $\iiint r^2 * \sin(\theta) dr d\theta d\varphi$  (see SunQM-3s3 for detailed explanation). Comparing Figure 2d to Figure 2a demonstrated that the calculated NBP density curve peaks are fatter than Born probability curve peaks. One way to avoid NBP's fat curve peak is that we may be able to use NBP's power index to narrow the peak. Again, we are not sure what the correct calculation should be. In columns 14 through 16 of Table 1, according to what we learned from SunQM-4 and SunQM-4s1, we simply changed  $\sin(\theta) \rightarrow \{[1 +$

$\sin(\theta)/2\}^n$ , or  $\cos(\theta) \rightarrow \{[1 + \cos(\theta)]/2\}^n$ , with  $n=8$ . Although the resulted Figure 2e did show NBP's curve peaks getting narrowed, but it moved  $|2,1,0\rangle$  QM state's NBP peaks too close to poles (if  $n$  keeps increasing). This means that we still need to figure out how to correctly calculate the NBP for the general  $|n,l,m\rangle$  QM states. After all, this NBP calculation is only a citizen scientist level's try, may or may not be correct.

As mentioned in SunQM-4s1 section V, an orbital moving planet's  $\theta$ -dimensional 1D matter wave is in a true standing wave mode. Using the same concept, we can conclude that the spinning Earth's  $\theta$ -dimensional 1D matter wave is also in a true standing wave mode. For a true standing wave, our result (in Figure 2) showed that Born probability description is better than NBP description because it generates relative sharp (and clear cut) curve peaks.

Table 1. Calculations of Born probability and NBP for Earth atmosphere's  $|2,1,0\rangle$  and  $|2,1,1\rangle$  QM states.

$\theta, \text{in } \pi$	$\theta, \text{in arc}$	$\theta', \text{in deg}$	3D projecte d to 2D	spin cause d $y\sin(\theta^*$ 1.0)	spin cause d $y\sin(\theta^*$ 0.9)	$\sin(\theta)^*$ $ Y(0,0) ^2$	$\sin(\theta)^*$ $ Y(1,0) ^2$	$\sin(\theta)^*$ $ Y(1,1) ^2$	NBP= $[1+\sin(\theta)]/2$				NBP= $[1+\sin(\theta)]/2^8$			
									$Y(0,0,\text{NB})$ P)	$Y(1,0,+\text{NB})$ NBP)	$Y(1,0,-\text{NB})$ NBP)	$Y(1,1,\text{NB})$ P)	$\sin(\theta)^*$ $Y(1,0,+\text{NB})$ NBP) <sup>n</sup>	$\sin(\theta)^*$ $Y(1,0,-\text{NB})$ NBP) <sup>n</sup>	$\sin(\theta)^*$ $Y(1,1,\text{NB})$ BP) <sup>n</sup>	$\sin(\theta)^*$ $Y(1,1,\text{NB})$ BP) <sup>n</sup>
0	0	90	1.000	1.000	0.988	0.000	0.000	0.000	0.000	0.000	0.000	0.000	0.000	0.000	0.000	
1/32	0.098	84	0.995	0.995	0.970	0.008	0.023	0.000	0.028	0.048	0.000	0.019	0.047	0.000	0.000	
1/16	0.196	79	0.981	0.981	0.945	0.016	0.045	0.002	0.055	0.094	0.001	0.040	0.088	0.000	0.001	
3/32	0.295	73	0.957	0.957	0.912	0.023	0.063	0.006	0.082	0.139	0.003	0.065	0.119	0.000	0.003	
1/8	0.393	68	0.924	0.924	0.872	0.030	0.078	0.013	0.108	0.180	0.007	0.091	0.137	0.000	0.007	
5/32	0.491	62	0.882	0.882	0.826	0.038	0.088	0.025	0.133	0.217	0.014	0.120	0.142	0.000	0.014	
3/16	0.589	56	0.831	0.831	0.773	0.044	0.092	0.041	0.157	0.249	0.023	0.149	0.134	0.000	0.026	
7/32	0.687	51	0.773	0.773	0.714	0.050	0.090	0.061	0.179	0.275	0.035	0.179	0.118	0.000	0.044	
1/4	0.785	45	0.707	0.707	0.649	0.056	0.084	0.084	0.199	0.295	0.051	0.209	0.097	0.000	0.069	
9/32	0.884	39	0.634	0.634	0.580	0.062	0.074	0.110	0.218	0.309	0.069	0.237	0.075	0.000	0.102	
5/16	0.982	34	0.556	0.556	0.506	0.066	0.061	0.137	0.235	0.316	0.090	0.263	0.054	0.000	0.142	
11/32	1.080	28	0.471	0.471	0.428	0.070	0.047	0.164	0.249	0.317	0.114	0.287	0.037	0.000	0.187	
3/8	1.178	23	0.383	0.383	0.346	0.074	0.032	0.188	0.261	0.312	0.139	0.307	0.024	0.000	0.234	
13/32	1.276	17	0.290	0.290	0.262	0.076	0.019	0.209	0.270	0.302	0.166	0.323	0.014	0.000	0.278	
7/16	1.374	11	0.195	0.195	0.176	0.078	0.009	0.225	0.277	0.286	0.193	0.336	0.008	0.000	0.314	
15/32	1.473	6	0.098	0.098	0.088	0.079	0.002	0.235	0.281	0.267	0.219	0.343	0.004	0.001	0.337	
1/2	1.571	0	0.000	0.000	0.000	0.080	0.000	0.239	0.282	0.244	0.244	0.345	0.002	0.002	0.345	
17/32	1.669	-6	-0.098	-0.098	-0.088	0.079	0.002	0.235	0.281	0.219	0.267	0.343	0.001	0.004	0.337	
9/16	1.767	-11	-0.195	-0.195	-0.176	0.078	0.009	0.225	0.277	0.193	0.286	0.336	0.000	0.008	0.314	
19/32	1.865	-17	-0.290	-0.290	-0.262	0.076	0.019	0.209	0.270	0.166	0.302	0.323	0.000	0.014	0.278	
5/8	1.963	-23	-0.383	-0.383	-0.346	0.074	0.032	0.188	0.261	0.139	0.312	0.307	0.000	0.024	0.234	
21/32	2.062	-28	-0.471	-0.471	-0.428	0.070	0.047	0.164	0.249	0.114	0.317	0.287	0.000	0.037	0.187	
11/16	2.160	-34	-0.556	-0.556	-0.506	0.066	0.061	0.137	0.235	0.090	0.316	0.263	0.000	0.054	0.142	
23/32	2.258	-39	-0.634	-0.634	-0.580	0.062	0.074	0.110	0.218	0.069	0.309	0.237	0.000	0.075	0.102	
3/4	2.356	-45	-0.707	-0.707	-0.649	0.056	0.084	0.084	0.199	0.051	0.295	0.209	0.000	0.097	0.069	
25/32	2.454	-51	-0.773	-0.773	-0.714	0.050	0.090	0.061	0.179	0.035	0.275	0.179	0.000	0.118	0.044	
13/16	2.553	-56	-0.831	-0.831	-0.773	0.044	0.092	0.041	0.157	0.023	0.249	0.149	0.000	0.134	0.026	
27/32	2.651	-62	-0.882	-0.882	-0.826	0.038	0.088	0.025	0.133	0.014	0.217	0.120	0.000	0.142	0.014	
7/8	2.749	-68	-0.924	-0.924	-0.872	0.030	0.078	0.013	0.108	0.007	0.180	0.091	0.000	0.137	0.007	
29/32	2.847	-73	-0.957	-0.957	-0.912	0.023	0.063	0.006	0.082	0.003	0.139	0.065	0.000	0.119	0.003	
15/16	2.945	-79	-0.981	-0.981	-0.945	0.016	0.045	0.002	0.055	0.001	0.094	0.040	0.000	0.088	0.001	
31/32	3.043	-84	-0.995	-0.995	-0.970	0.008	0.023	0.000	0.028	0.000	0.048	0.019	0.000	0.047	0.000	
1	3.142	-90	-1.000	-1.000	-0.988	0.000	0.000	0.000	0.000	0.000	0.000	0.000	0.000	0.000	0.000	

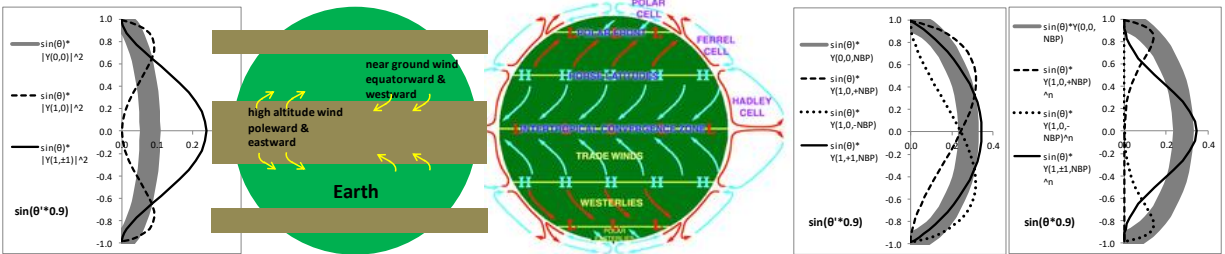


Figure 2a (left No. 1). Born probability of  $\sin(\theta)*|Y(l=1,m)|^2$  (and  $\sin(\theta)*|Y(0,0)|^2$ ) vs.  $\sin(\theta^*0.9)$ .  
 Figure 2b (left No. 2). Simplified Figure 2c by extending (the band) of peaks to the front of a ball that pretend to be Earth.  
 Figure 2c (left No. 3). An idealized view of three large circulation cells in Earth's atmosphere. (Copied from wiki "Atmosphere of Earth", [https://en.wikipedia.org/wiki/Atmosphere\\_of\\_Earth](https://en.wikipedia.org/wiki/Atmosphere_of_Earth). Author: DWindrim. Copyright: CC BY-SA 3.0)  
 Figure 2d (left No. 4). NBP plot for:  $Y(1,0,+NBP) * \sin(\theta) = 1/2 * \sqrt{3/\pi} * [(1 + \cos(\theta))/2 * \sin(\theta)]$ ; and  $Y(1,0,-NBP) * \sin(\theta) = 1/2 * \sqrt{3/\pi} * [(1 + \cos(\pi-\theta))/2 * \sin(\theta)]$ ; and  $Y(1,1,NBP) * \sin(\theta) = 1/2 * \sqrt{3/2/\pi} * [(1 + \sin(\theta))/2 * \sin(\theta)]$ .  
 Figure 2e (left No. 5). NBP plot for:  $[Y(1,0,+NBP)^n] * \sin(\theta) = 1/2 * \sqrt{3/\pi} * \{[(1 + \cos(\theta))/2]^8 * \sin(\theta)\}$ ; and  $[Y(1,0,-NBP)^n] * \sin(\theta) = 1/2 * \sqrt{3/\pi} * \{[(1 + \cos(\pi-\theta))/2]^8 * \sin(\theta)\}$ ; and  $[Y(1,1,NBP)^n] * \sin(\theta) = 1/2 * \sqrt{3/2/\pi} * \{[(1 + \sin(\theta))/2]^8 * \sin(\theta)\}$ .

### I-c. Using the spinning $\{N,n\}$ QM to explain Earth atmosphere's jet streams

As wiki "Jet stream" explained, "*Jet streams are fast flowing, narrow, meandering air currents in the atmospheres*" of Earth. The (stronger) polar jets locate at  $\sim 60^\circ$  latitude and 9 ~ 12 km above sea level, and the (weaker) subtropical jets locate at  $\sim 30^\circ$  latitude and 10 ~ 16 km above sea level (see Figure 3). Recall that  $r_n = r_1 * n^2$ , so  $r/r_1 = 4$  means  $n^2 = 4$ , or  $n=2$ , and  $r/r_1 = 9$  means  $n=3$ . Also recall the rule of "all mass (or space) between  $r_n$  and  $r_{n+1}$  belongs to orbit  $n$ " (see SunQM-3s2 section IV). Figure 4a showed that the Born probability radial distribution for the  $n=2$  shell space (mainly from  $r/r_1 = 4$  to  $r/r_1 = 9$ , including both  $l=0$  and  $l=1$  sub-shells, with the  $r$ -dimensional probability density function  $r^2 * |R(n=2,l)|^2$ ), and for the  $n=3$  shell (mainly from  $r/r_1 = 9$  to  $r/r_1 = 16$ , including  $l=0, l=1$  and  $l=2$  sub-shells, with the  $r$ -dimensional probability density function  $r^2 * |R(n=3,l)|^2$ ). Now let's study it one-by-one:

1) First let's analyze the  $n=2$  shell. We see that  $r^2 * |R(2,1)|^2$  probability curve's peak is at  $r/r_1 = 4$ , and  $r^2 * |R(2,0)|^2$  curve's peak is at  $r/r_1 \approx 5$ , revealing  $|2,0,0\rangle$  or  $l=0$  sub-shell is at the outside of  $|2,1,m\rangle$  or  $l=1$  sub-shell. Similarly, for the  $n=3$  shell, the  $l = 2, 1, 0$  sub-shells are lined-up one-by-one approximately from  $r/r_1 = 9$  at inner to  $r/r_1 = 16$  at outer.

2) Now let's analyze the  $n=2$ 's  $l=0$  sub-shell (see  $r/r_1$  range from  $\approx 5$  to  $\approx 9$  in Figure 4a). Its  $r$ -probability is dominated by  $r^2 * |R(2,0)|^2$  or  $|2,0,0\rangle$ , with some  $r^2 * |R(2,1)|^2$  or  $|2,1,m\rangle$ , and a small amount of  $r^2 * |R(3,2)|^2$  or  $|3,2,m\rangle$ . There are negligible amount of  $r^2 * |R(3,1)|^2$  or  $|3,1,m\rangle$  and  $r^2 * |R(3,0)|^2$  or  $|3,0,0\rangle$ , and they can be ignored. This means at the outer edge of  $|2,0,0\rangle$  sub-shell, we will see small amount of  $|3,2,m\rangle$  QM state with  $m=2, 1, 0$ .

3) Figure 4b showed that for the  $r^2 * |R(3,2)|^2$  or  $|3,2,m\rangle$ , or  $r^2 * |R(3,2)|^2 * |Y(l=2,m=(2,1,0))|^2$  probabilities, the corresponding  $|Y(2,0)|^2$  probability have peaks at around  $60^\circ$  latitude (where polar jets located), the corresponding  $|Y(2,1)|^2$  probability have peaks at around  $30^\circ$  latitude (where subtropical jets located), and corresponding  $|Y(2,2)|^2$  probability has a peak at  $\sim 0^\circ$  latitude (where no jet has been found). Notice that the three (red) curves of  $|Y(l=2,m=(2,1,0))|^2$  in Figure 4b correspond to the single red curve in Figure 4a.

4) As mentioned in section I-a, we can reasonably guess that due to too little air mass, the effective thickness of Earth atmosphere's  $n=2$  shell is suppressed to between the sea level and 12 km above sea level. We can further assume that the troposphere (from 0 km to 10 km above sea level) belongs to  $|2,1,m\rangle$  or  $l=1$  sub-shell, and the tropopause (from 10 km to 12 km above sea level) belongs to  $|2,0,0\rangle$  or  $l=0$  sub-shell (see the illustration in Figure 3 for troposphere, tropopause, and stratosphere). Note: at the equator, troposphere may change to 0 ~ 13 km, and tropopause 13 ~ 16 km.

5) In Figure 3, if we simplify to that troposphere has 50%~100% mass occupancy, tropopause has ~25% mass occupancy, and stratosphere has ~0% mass occupancy, then we can describe the polar jets as the small amount of air mass in  $|3,2,0\rangle$  QM state, embedded at the outer edge of  $|2,0,0\rangle$  sub-shell (equivalent to the top-end of the tropopause), and formed zonal band at  $\sim 60^\circ$  latitude. Similarly, we can describe the subtropical jets as the small amount of air mass in  $|3,2,1\rangle$  QM state, embedded at the outer edge of  $|2,0,0\rangle$  sub-shell (equivalent to the top-end of the tropopause), and formed zonal band at  $\sim 30^\circ$  latitude. This  $\{N,n\}$  QM description well matches polar jets' and subtropical jets' altitude and latitude. Note: that the residue  $|3,2,m\rangle$  zonal bands embedded in the outer edge of  $|2,0,0\rangle$  shell space only become possible when in the outer space of  $|2,0,0\rangle$ , or in the  $|3,l,m\rangle$  shell space, the mass occupancy  $\approx 0\%$ . For better understanding, check the explanation of SunQM-3s3's Figure 4, where the residue  $|5,4,m\rangle$  zonal bands embedded in the outer edge of  $|4,0,0\rangle$  shell space, because Jupiter surface is at the outer edge of  $|4,0,0\rangle$ , and outer of  $|4,0,0\rangle$  shell space (or in the  $|5,4,m\rangle$  shell space) the mass occupancy  $\approx 0\%$ .

6) Furthermore, according to the same analysis, there should be a small amount of air mass in  $|3,2,2\rangle$  QM state, embedded at the outer edge of  $|2,0,0\rangle$  sub-shell (equivalent to the top-end of the tropopause), and formed zonal band at  $\sim 0^\circ$  latitude (see the yellow circles in Figure 3). However, there is no polar/subtropical jets equivalent jet has been reported near equator. One possible explanation is that the strong nLL QM effect at equator pushes  $|2,0,0\rangle$  sub-shell much out to  $> 30$  km above the sea

level, where the air mass density is  $\ll 1\%$  of the sea level's air mass density, so that the jet at  $0^\circ$  latitude is no longer obvious.

Figure 3 was drawn based on wiki "Jet stream" figure "Cross section of the subtropical and polar jet streams by latitude" with many modifications. According to the above  $\{N,n\}$  QM modeling results, we added: troposphere = active  $|2,1,m\rangle$  shell, tropopause = active  $|2,0,0\rangle$  shell, stratosphere = active  $|3,2,m\rangle$  shell, Polar Jet = active residue  $|3,2,0\rangle$  zonal band embedded in the active  $|2,0,0\rangle$  outer surface, Subtropical Jet = active residue  $|3,2,1\rangle$  zonal band embedded in the active  $|2,0,0\rangle$  outer surface. Furthermore, because at the interface between warm air and cold air, the warm air always climbs on top of the cold air (by the classical physics), so that it will form a sharp turning corner ( $< 90^\circ$ , notice this is a square-shape corner's geometric degree) in Hadley/Ferrel circulation cells. We guess that (in the classical physics) both jets may be generated by this sharp corner turning in circulation cell, so that the Polar jet stream may have clockwise rolling along the stream, and the Subtropical jet stream may have anticlockwise rolling along the stream (as shown in Figure 3).

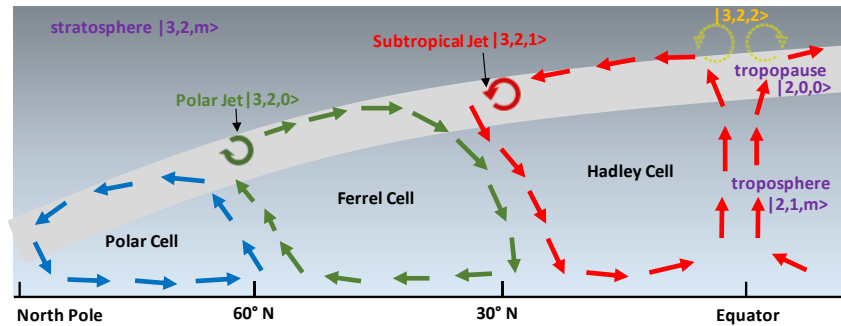


Figure 3. Cross section of the subtropical and polar jet streams by latitude, explained with  $\{N,n\}$  QM analysis.

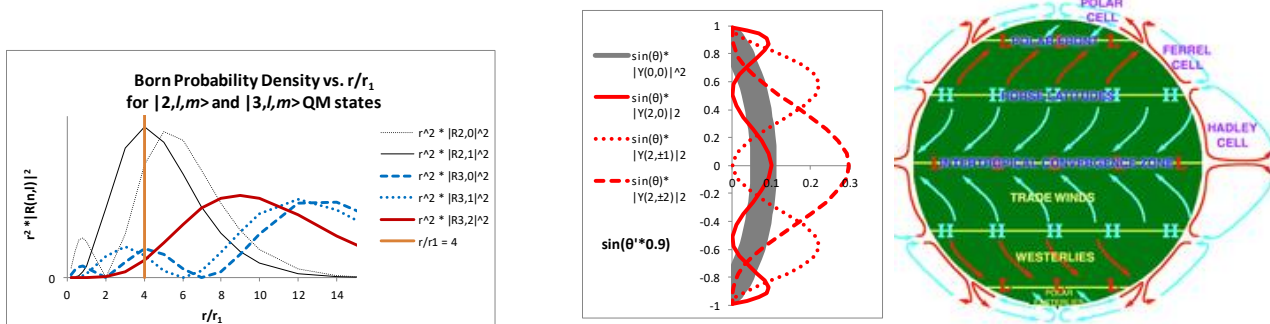


Figure 4a (left). Born probability  $r$ -dimensional density curve for  $|2,l,m\rangle$  and  $|3,l,m\rangle$ .

Figure 4b (middle). Born probability  $\theta$ -dimensional density curve for  $|3,l=2,m(=0,1,2)\rangle$ .

Figure 4c (right). Same as Figure 2c.

**I-d. Is QM force (or thermal force) the primary force to form Hadley/Ferrel/Polar three cells?**

Most text books say that the thermal force is the primary force to form Hadley/Ferrel/Polar three circulation cells. For example, wiki "Atmospheric circulation" mentioned that "Though the Hadley cell is described as located at the equator, in the northern hemisphere it shifts to higher latitudes in June and July and toward lower latitudes in December and January, which is the result of the Sun's heating of the surface. The zone where the greatest heating takes place is called the thermal equator". However, in SunQM-3s3 and in the current paper, we suggest that the QM force is the primary force for forming Hadley/Ferrel/Polar cells based on the following three reasons:

- 1)  $\{N,n\}$  QM can explain Earth atmosphere's elliptical shape, the Hadley/Ferrel/Polar three global circulation cells with interfaces at  $30^\circ$  and  $60^\circ$  latitude, the polar jets at the high altitude of  $60^\circ$  latitude, and the subtropical jets at the high altitude

of 30° latitude, all together with a single theory and calculation. In this theory, Earth atmosphere's up-welling forces at both 0° and 60° latitude are caused by the QM's mass-peaking effect, and the down-welling forces at both 30° and 90° latitude are caused by the QM's mass-depleting effect. If the thermal force is the primary force to form Hadley/Ferrel/Polar cells, then we should have seen that the major up-welling site of the air at equator should closely follow the "thermal equator", and Earth atmosphere's elliptical shape should also change seasonally according the "thermal equator". However, we haven't seen this kind of report.

2)  $\{N,n\}$  QM can also explain Jupiter atmosphere's global circulation (see SunQM-3s3 section I). As wiki "Atmosphere of Jupiter" mentioned that "Zones, which are colder than belts, correspond to upwellings, while belts mark descending air", so the thermal force is not the primary force for Jupiter atmosphere surface's global circulation.

3) As wiki "Weather" mentioned that "The weather is ultimately created by solar energy and the amount of energy received by Neptune is only about 1/900 of that received by Earth, yet the intensity of weather phenomena on Neptune is far greater than on Earth. ... This has created a puzzle for planetary scientists".  $\{N,n\}$  QM can be used to explain any planet (including Neptune) atmosphere's global circulation.

Therefore, we believe that the QM force is the primary force to form Hadley/Ferrel/Polar cells, and the thermal force is the secondary force that modulate the primary QM force and cause "thermal equator" shift on Earth.

## II. Using $Y(l,m)$ based NBP to describe a hurricane related low mass density center (or a low air pressure center) in atmosphere

In section I, we have successfully used  $\{N,n\}$  QM's  $\theta$ -1D Born probability (and NBP) to explain Earth's global atmospheric phenomenon, including its elliptical shape, the Hadley/Ferrel/Polar three global circulation cells, and the jets streams. In the current section, we are going to use  $\{N,n\}$  QM's  $Y(l,m)$  related probability to explain Earth's local atmospheric phenomenon (e.g., a low air mass density center for the hurricane formation). We cannot use Born probability for the explanation because that for a  $|n,l,m\rangle$  QM state, the traditional Born probability's conjugated-square of  $|Y(l,m)|^2$  will cancel out all  $\phi$ -dimension's information (see John S. Townsend, A Modern Approach to Quantum Mechanics, 2nd ed., 2012, page 335, Figure 9.11). Therefore, we can only use NBP to describe Earth's  $\theta\phi$ -2D related atmospheric local phenomenon if we want to retain the  $\phi$ -dimension's information. However, in SunQM-4 and SunQM-4s1, we only showed that NBP is valid for  $|nLL\rangle$  QM state. So here we need to assume that, 1) NBP is also valid for all  $|n,l,m\rangle$  QM states besides the  $nLL$  QM state (Note: in SunQM-3s11 section II-c's eq-31 through eq-37, we may have proved this); 2) the  $\theta\phi$ -2D NBP can also be calculated as to lift-up the  $Y(l,m)$  function (e.g., the real part of  $Y(l,m)$ , on a baseline curve) so that its  $\text{Re}[Y(l,m)]$  negative amplitude peak become NBP density's minimum value ( $=0$ ), and then divided by 2 so that the lifted  $\text{Re}[Y(l,m)]$  function's positive amplitude peak become NBP density's maximum value ( $=1$ ), which is similar as the NBP calculation for  $|nLL\rangle$  QM states. (Note: at this time, we are unable to prove this assumption mathematically, so the whole section II is a citizen scientist leveled analysis at this time).

In section I, we have described Earth atmosphere by using the base QM mode  $|2,l=1,m\rangle$  with  $r_1$  or  $p\{0,1//2\}$  at Earth's inner core (or  $1/4$  of Earth's radius). According to  $\{N,n/q\}$  QM theory, we can move  $r_1$  inward or outward (by changing the  $N$  quantum number). For example, if we first set Earth surface  $r = 6.38E+6$  m as  $p\{0,1//2\}$  and as  $r_1$ , then move  $r_1$  inward to  $p\{-4,1//2\} = p\{0,1/16//2\}$  and reset it as  $r_1$ , and rename it as  $_{\text{new-}p}\{0,1//2\}$ , then Earth's radius has size of  $_{\text{new-}p}\{4,1//2\} = _{\text{new-}p}\{0,16//2\}$ , and then Earth atmosphere is in the  $_{\text{new-}p}\{0,16//2\}$  orbital shell space, and it should be described as  $|n,l,m\rangle = |16,l,m\rangle$  QM state. Since  $l = 0, \dots, n-1$ , so the maximum  $l = 16-1 = 15$ . According to SunQM-3s3's result, for  $n=16$  shell, there are 16 of  $l$  sub-shells (for  $l = 0, \dots, n-1$ ), and the  $l=15$  sub-shell is the inner most sub-shell. According to SunQM-3s1's result, for  $n=16$  shell in the spinning-reference frame,  $l=15$  sub-shell has the lowest state energy among all 16 ( $l = 0, \dots, 15$ ) sub-shells. So now we can use  $|n,l,m\rangle = |16,15,m\rangle$  QM state (instead of  $|2,1,m\rangle$  QM state in section I) to describe Earth's atmosphere. Its NBP density is directly correlate to the real part of  $R(n=16,l=15) * Y(l=15,m)$ . In Figure 5, we plotted out three of  $m$  states for  $\text{Re}[Y(l=15,m=15)]$ ,  $\text{Re}[Y(l=15,m=7)]$ , and  $\text{Re}[Y(l=15,m=2)]$ . According to  $Y(l,m)$ 's rule (see wiki "spherical harmonics" section "Visualization of the spherical harmonics"), "The Laplace spherical harmonics  $Y(l,m)$  can be visualized by considering their "nodal lines", that is, the set of points on the sphere where  $\text{Re}[Y(l,m)] = 0$  (or  $\text{Im}[Y(l,m)] = 0$ )". Each nodal line forms a circle, so for a  $Y(l,m)$ , there are total  $l$  nodal line circles. Among them, there are  $|m|$  nodal line circles

in parallel with  $z$  axis, and  $l-|m|$  nodal line circles in parallel with  $x$ - $y$  plane. For example,  $\text{Re}[Y(15,15)]$  has  $|m|=15$  nodal line circles in parallel with  $z$  axis, and  $l-|m|=0$  nodal line circles in parallel with  $x$ - $y$  plane (see Figure 5a),  $\text{Re}[Y(15,7)]$  has  $|m|=7$  nodal line circles in parallel with  $z$  axis, and  $l-|m|=8$  nodal line circles in parallel with  $x$ - $y$  plane (see Figure 5b), and  $\text{Re}[Y(l=15,m=2)]$  has  $|m|=2$  nodal line circles in parallel with  $z$  axis, and  $l-|m|=13$  nodal line circles in parallel with  $x$ - $y$  plane (see Figure 5c).

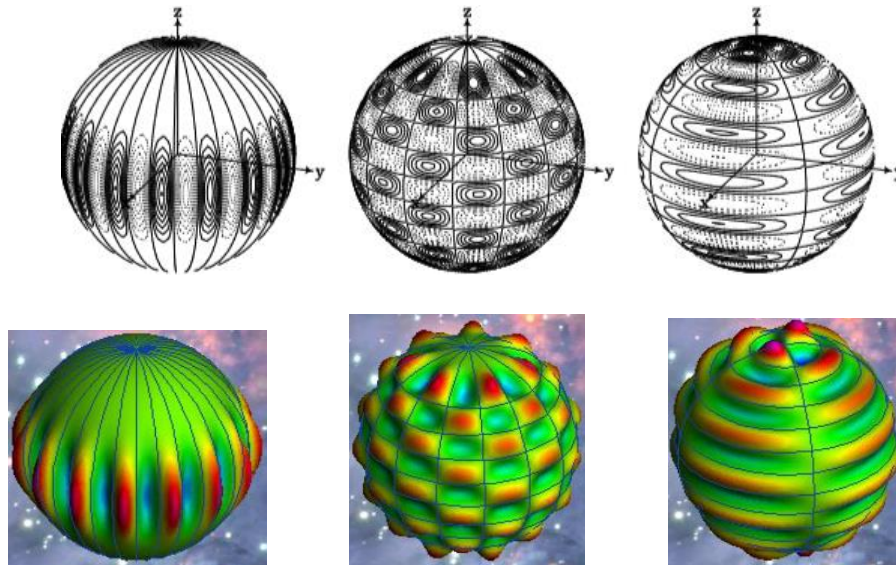


Figure 5 (a, b, c, top left, top middle, and top right). Spherical contour plot of  $\text{Re}[Y(l=15,m=15)]$ ,  $\text{Re}[Y(l=15,m=7)]$ , and  $\text{Re}[Y(l=15,m=2)]$ . Copied from the QM text book by James Binney & David Skinner, *The Physics of Quantum Mechanics*, 1st ed. 2014. p133, Figure 7.4. Copy permission: granted by the original author.

Figure 5 (d, e, f, bottom left, bottom middle, and bottom right). Spherical surface (or solid) plot of  $\text{Re}[Y(15,15)]$ ,  $\text{Re}[Y(15,7)]$ , and  $\text{Re}[Y(15,2)]$ . Plotted by using the (free) online plotter at "<http://icgem.gfz-potsdam.de/vis3d/tutorial>".

For any single  $l$  value, we know that after summing all Born probability  $|Y(l,m)|^2$  for  $m = -l, \dots, +l$ , we obtain a perfect sphere (i.e., a probability =1 sphere in a spherical 3D plot). So if we use  $|Y(l=15,m)|^2$  to describe a non-spin Earth atmosphere, after summed all  $m = -15 \dots +15$ , it will be a perfect sphere. For a spinning Earth, we know that Figure 5a's  $Y(15,15)$  is at the nLL QM state, and has the lowest state energy  $E$  (among all possible  $m = -15 \dots +15$  QM states), so the air mass is populated the most. Also Figure 5c's  $Y(15, 2)$  has the smallest  $m$  among all three plots, so it has the highest  $E$ , and the air mass is the least populated among all three QM states in Figure 5. So (besides a spinning  $|2,1,1\rangle$  QM model), using a spinning  $|16,15,m\rangle$  QM model, we can also describe an elliptical (or M&M candy) shaped Earth atmosphere. Although to describe Hadley/Ferrey/polar cells, using  $|2,1,1\rangle$  QM model is much better than to use  $|16,15,m\rangle$  QM model.

Now with  $|16,15,m\rangle$  QM mode alone (or with  $|2,1,m\rangle$  QM mode alone) and with all  $m$  values perfectly distributed, we can have a perfect spherical atmosphere (for a non-spin Earth), but standing still, without any local weather. After adding spin to Earth (which generates QM's nLL effect), it re-shapes the atmosphere into an elliptical shape, and produced Hadley/Ferrey/polar cells (the global atmosphere circulation), but still there is not much local weather. Then we add the quantum fluctuation to the  $l$  and  $m$  value's distribution (to make their distribution away from the perfect), the noisy imperfectness will produce the local weather. This is like (using Fourier transformation) with a perfect spectrum of sine waves we can make a perfect straight line, and by introducing the noisy imperfectness it will produce the local noise out of a perfect straight line.

According to wiki "weather", "*Weather is driven by air pressure, temperature and moisture differences between one place and another*". The mass density (or the air mass density, which is directly correlate to the QM probability density) differences between one place and another is one of the most important factors to generate the (air) pressure differences. Now let's find a weather phenomenon that is directly caused by the local air mass density is either too high or too low. From text

books, we know that a tropic cyclone or a hurricane is formed around an abnormally low air pressure center (which is directly generated by the low air mass density as the result of the warm air rising). For example, wiki "Hurricane Dorian" mentioned that "Dorian developed from a tropical wave on August 24 over the Central Atlantic. ... proceeded to undergo rapid intensification over the following days to reach its peak as a Category 5 hurricane with ... a minimum central pressure of 910 millibars (910 hPa) by September 1". On ~ 8/25/2019, right before the hurricane Dorian was formed, it had a low air pressure (~1010 hPa) center at Atlantic Ocean (~10°N and ~51°W) surrounded by the normal sea-level air pressure ~1013 hPa (see

[https://earth.nullschool.net/#2019/08/25/0700Z/wind/surface/level/overlay=mean\\_sea\\_level\\_pressure/orthographic=-44.11,13.19,373/loc=-51.161,10.555](https://earth.nullschool.net/#2019/08/25/0700Z/wind/surface/level/overlay=mean_sea_level_pressure/orthographic=-44.11,13.19,373/loc=-51.161,10.555), figure not shown here). Now if we can use  $\text{Re}[Y(l,m)]$ , or a combination of them, to

model out a single low mass density center at the position of ~10°N and ~51°W, then it means that we can use  $\{N,n\}$  QM's NBP to describe the initial formation of hurricane Dorian on ~ 8/25/2019 (because NBP directly correlate to the real part of the wave function  $\text{Re}[Y(l,m)]$ ). Can we do it? The answer is "yes".

Previously we have mentioned to use a spinning  $|16,15,m\rangle$  QM model, or  $\text{Re}[Y(15,m)]$  wave function to describe Earth's atmosphere. Now we can rephrase the question as: how to use a spinning  $|16,15,m\rangle$  QM model, or  $\text{Re}[Y(15,m)]$  wave function to describe Earth atmosphere's one single low mass density center at ~10°N and ~51°W (to mimic the pre-hurricane Dorian on ~ 8/25/2019)? In SunQM-3s11, we have showed that for nLL QM state in  $\phi$ -1D dimension, how to use  $\text{Re}[Y(l,m)] \propto \cos(m*\phi) * \sin(\theta)^l$  with  $l = m = n-1$ , and how to change its probability in  $\phi$ -1D dimension from the multiple peaks with "flat" distribution to a single peak by using a combination of  $\text{Re}[Y(l,m+\delta)]$  with  $m = 1024$  and  $\delta = -36, \dots +36$ . Here we use the same method but expanded it from  $\phi$ -1D to  $\theta\phi$ -2D dimension. To do this, we need to sum not only many different  $m(s)$ , but also many different  $l(s)$  for  $\text{Re}[Y(l,m)]$  as shown in eq-1.

$$\sum_l \sum_m \text{Re}[Y(l,m)]$$

eq-1

In our special case for the  $|16,15,m\rangle$  QM state, we need  $l$  range from less than 15 to larger than 15, and  $m = -l, \dots +l$  for every single  $l$ .

However, as a citizen QM scientist, I don't have the resource to obtain  $Y(l,m)$  analytical formulas with  $l > 10$ . The only resource I have is wiki "Tables of Spherical Harmonics", where  $Y(l,m)$  formulas of  $l \leq 10$  are listed. So we can only use low  $l$  quantum number ( $\leq 10$ ) for the calculation of eq-1. Luckily, we had discovered one of the natural attributes of  $\{N,n\}$  QM, that is "Simultaneous-Multi-Eigen-Description (SMED)" (see SunQM-4 section V, and also see a future paper SunQM-4s6). With the concept of SMED, we can use a combination of low  $l$   $Y(l,m)$  for the calculation of eq-1 to obtain the low resolution result. It is just like a small piece of a holograph will give the same whole picture as the large one, but with much lower resolution. Also, as a citizen QM scientist, I don't have any sophisticated software either to calculate eq-1, or to plot the result, so I can only use Microsoft Excel spreadsheet to calculate eq-1, and to present the result graphically by directly showing the (color contoured) Excel spreadsheet (as shown in Figure 6).

Figure 6a showed a  $\theta\phi$ -2D contour map of the real part of spherical harmonics  $\text{Re}[Y(10,4)]$ . The red contour represents the positive amplitude peak (at cut-off  $> 0.3$ ), and blue contour represents the negative amplitude peak (at cut-off  $< -0.3$ ). It showed +/- peaks spread everywhere in  $\theta\phi$ -2D dimension. In Figure 6b, after summing  $\text{Re}[Y(10,4) - Y(9,3) + Y(8,2)]/3$ , we see those +/- peaks away from  $\phi=0$  are significantly suppressed. Notice that we did this by choosing  $m=4, 3, 2$  in three  $\text{Re}[Y(l,m)]$  functions so that the different spacial frequencies of  $m(s)$  in  $\phi$ -dimension are suppressing with each other. We also keep  $l-|m|=6$  for all three  $Y(l,m)$  and choose the appropriate + or - sign for summing, so that each of these three  $\text{Re}[Y(l,m)]$  functions always has negative peak at  $\theta=90^\circ$  and  $\phi=0^\circ$  position (and this is the low probability density center we try to build up for the hurricane). In Figure 6c, after summing  $\text{Re}[Y(10,4) - Y(9,3) + Y(8,2)]/3 + \text{Re}[-Y(10,6)+Y(9,5)-Y(8,4)]/3 + \text{Re}[Y(10,8)-Y(9,7)+Y(8,6)]/3 + \text{Re}[-Y(10,10)+Y(9,9)-Y(8,8)]/3$ , we see that only the negative peak at  $\theta=90^\circ$  and  $\phi=0^\circ$  position is retained, and the +/- peaks at all other  $\theta\phi$  positions are (relatively) suppressed. Again, we did this by choosing  $l-|m|$  at different values so that the different spacial frequencies of  $l-|m|$  in  $\theta$ -dimension are suppressing with each other.

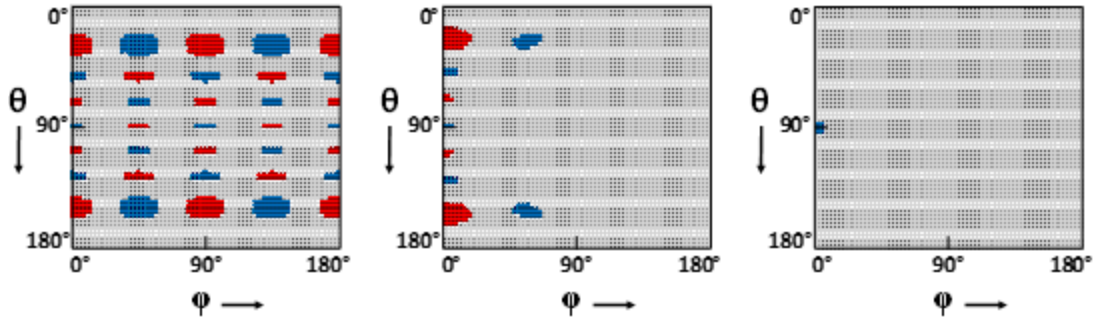


Figure 6a (left).  $\theta\phi$ -2D contour map of spherical harmonics  $\text{Re}[Y(l=10,m=4)]$ . For all three figures, red contour represents the positive amplitude peak (at cut-off  $> 0.3$ ), and blue contour represents the negative amplitude peak (at cut-off  $< -0.3$ ). Microsoft Excel spreadsheet is used for both the spherical harmonics summing calculation and the graphic plot.  
 Figure 6b (middle).  $\theta\phi$ -2D contour map of  $\text{Re}[Y(10,4) - Y(9,3) + Y(8,2)]/3$ .  
 Figure 6c (right).  $\theta\phi$ -2D contour map of  $\text{Re}[Y(10,4) - Y(9,3) + Y(8,2)]/3 + \text{Re}[-Y(10,6)+Y(9,5)-Y(8,4)]/3 + \text{Re}[Y(10,8)-Y(9,7)+Y(8,6)]/3 + \text{Re}[-Y(10,10)+Y(9,9)-Y(8,8)]/3$ .

Because NBP directly correlates to the wave function, then NBP function's  $\theta\phi$ -2D contour map exactly follows the  $\text{Re}[Y(l,m)]$  wave function's  $\theta\phi$ -2D contour map (although the absolute values of two maps are different):  $\text{Re}[Y(l,m)]$  wave function's positive amplitude represents the air mass density that is above the averaged air mass density (which equals to  $1.225 \text{ kg/m}^3$ , at Earth sea level, at  $15^\circ\text{C}$ , and has air pressure  $1013 \text{ hPa}$ ), and  $\text{Re}[Y(l,m)]$  wave function's negative amplitude represents the air mass density below the averaged air mass density (see SunQM-4s1's Figure 10 for the 1D-QM explanation).

So in Figure 6c, we obtained a single negative  $\text{Re}[Y(l,m)]$  peak (which equivalent to a NBP minimum center, or a low air mass density center, or a low air pressure center) at  $\theta=90^\circ$  and  $\phi=0^\circ$  position. But we need it at position of  $\sim 10^\circ\text{N}$  and  $\sim 51^\circ\text{W}$  for the pre-hurricane Dorian. For a spinning Earth, we can reset the spherical coordinate to make  $\phi=0$  at  $51^\circ\text{W}$  longitude. But we can't do the same thing to shift  $\theta=90^\circ$  to  $10^\circ\text{N}$  latitude. Then, in construction of Figure 6b and Figure 6c, why don't we set the negative peak directly at  $10^\circ\text{N}$  latitude (and not at  $\theta=90^\circ$ ) at the beginning? We had tried that, while it intensifying the negative peak at  $10^\circ\text{N}$  latitude, it also intensified an either negative or positive peak at  $10^\circ\text{S}$  latitude simultaneously, and there is no way to eliminated the 2<sup>nd</sup> (and unwanted) peak. The only way to make a single (negative) peak in  $\theta$ -dimension by summing  $\text{Re}[Y(l,m)]$  is to make it at  $\theta=90^\circ$  (simply because all  $\text{Re}[Y(l,m)]$  functions have a  $+/+$  or  $+/-$  symmetry along x-y plane). Then how do we shift the single negative  $\text{Re}[Y(l,m)]$  peak from  $\theta=90^\circ$  to  $10^\circ\text{N}$  latitude? The answer is: through the thermal equator (see wiki "thermal equator"). In the hurricane season, Earth's thermal equator moves up to  $\sim 10^\circ\text{N}$  latitude rather than Earth's geographic equator  $\theta=90^\circ$ . Here we have to assume that the  $Y(l,m)$  function (for Earth atmosphere description) have its "active  $\theta=90^\circ$ ", or the  $+/+$  (and/or the  $+/-$ ) symmetric x-y plane follows Earth's thermal equator rather than Earth's geographic equator. So at the (northern hemisphere) summer, when Earth's thermal equator moves up to  $\sim 10^\circ\text{N}$  latitude, the  $Y(l,m)$  function of Earth atmosphere's "active  $\theta=90^\circ$ " also moves to  $\sim 10^\circ\text{N}$  latitude, the whole original  $Y(l,m)$  function of  $0^\circ < \theta < 90^\circ$  is now compressed into  $0^\circ < \theta < \sim 80^\circ$  latitude range (we name it as the "active  $Y(l,m)$  function"), and the whole original  $Y(l,m)$  function of  $90^\circ < \theta < 180^\circ$  is now expanded into  $\sim 80^\circ < \theta < 180^\circ$  latitude range for this "active  $Y(l,m)$  function". In this way, we have built a single negative  $\text{Re}[Y(l,m)]$  peak (which equivalent to a NBP minimum center) at the "active  $\theta=90^\circ$  and  $\phi=0^\circ$ " position, which is at the true geographic position of  $\sim 10^\circ\text{N}$  and  $\sim 51^\circ\text{W}$ .

Besides following the seasonal change of Earth's thermal equator, Earth atmosphere's "active  $Y(l,m)$  function" should also follow Earth's continental distribution, the terrain change, etc. Then we can use the sum of these "active  $Y(l,m)$  functions" to construct a single negative  $\text{Re}[Y(l,m)]$  peak at any  $\theta$  (which means we no longer have to set the initial NBP low mass center at "active  $\theta=90^\circ$ "). This is useful to construct the winter storms that usually happened at  $40^\circ\text{N} \sim 50^\circ\text{N}$  latitude. Of course, as a citizen scientist, I am unable to build a real example of the "active  $Y(l,m)$  functions" and summing them (because it is too complicated for me). But in theory, it is doable. We can further assume that the original  $\text{Re}[Y(l,m)]$  has 90% weight (which determines the Earth atmosphere's elliptical shape and the normal sea-level air pressure =  $1013 \text{ hPa}$

globally), while the “active  $Y(l,m)$ ” has 10% weight (which determines the air pressure  $1013 \pm 100$  hPa locally). Furthermore, once we sum a lot of “active”  $Y(l,m)$  functions with much higher  $l$  ( $\gg 10$ ) and  $m$  values, we will obtain much accurate  $\text{Re}[Y(l,m)]$  wave function  $\theta\phi$ -2D contour map at high resolution.

### III. NBP analysis for the extreme weather: from hurricane array to the extreme quantum weather

Figure 7 showed a number of extreme weather conditions caused by hurricane arrays. Figures 7a and 7b showed that on 9/8/2017, a hurricane array made of Katia (left), Irma (center), and Jose (right), each apart by  $\sim 20^\circ$  longitude, was at the Gulf of Mexico and Caribbean Sea. Figures 7c and 7d showed that on 7/24/2017, a hurricane array made of tropical Storms Greg (left), Irwin (center), and hurricane Hilary (right), each apart by  $\sim 15^\circ$  longitude, was spanning at the East Pacific. Figure 7e showed that three tropical cyclones of the 2006 Pacific typhoon season at different stages of development at the West Pacific. With the knowledge of section II, we can describe them by using NBP, or (a combined)  $\text{Re}[Y(l,m)]$  wave functions'  $\theta\phi$ -2D contour map with three low negative centers (at least at citizen scientist level, meaning that in theory it is doable, but practically we are far from that).

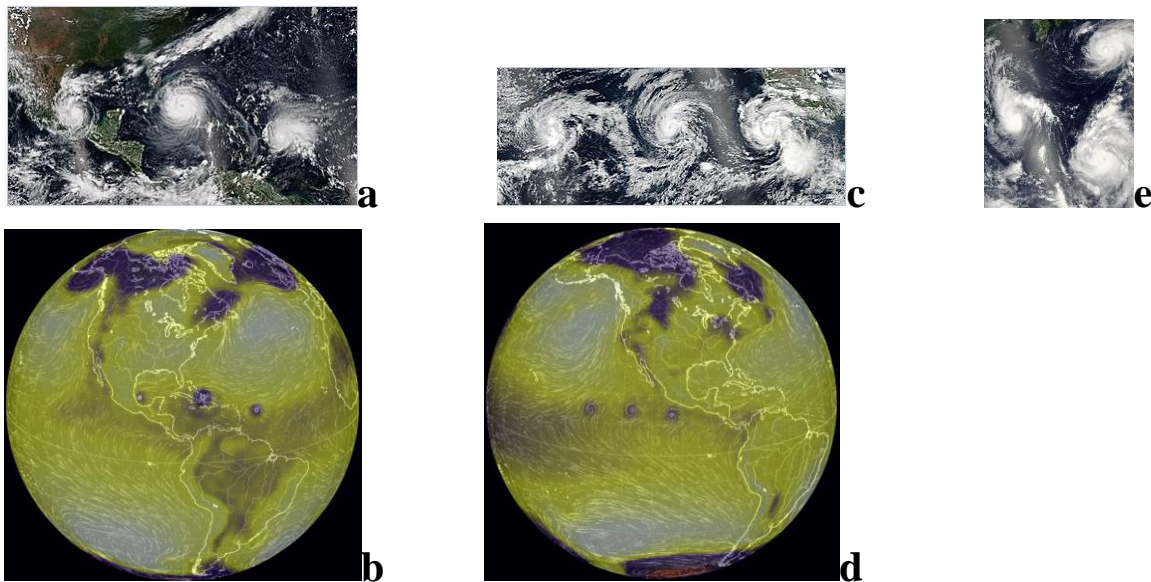


Figure 7a (top-left). Three simultaneous hurricanes active on 9/8/2017, with Katia (left), Irma (center), and Jose (right), copied from wiki “2017 Atlantic hurricane season”, [https://en.wikipedia.org/wiki/2017\\_Atlantic\\_hurricane\\_season](https://en.wikipedia.org/wiki/2017_Atlantic_hurricane_season), by the National Oceanic and Atmospheric Administration's Suomi NPP satellite. Copyright: Public domain.

Figure 7b (bottom-left). The corresponding global view of Figure 7a at the website of “earth :: a global map of wind, weather, and ocean conditions” at “<https://earth.nullschool.net/>”, at URL of

[https://earth.nullschool.net/#2017/09/08/0700Z/wind/surface/level/overlay=mean\\_sea\\_level\\_pressure/orthographic=-80.46,19.23,328](https://earth.nullschool.net/#2017/09/08/0700Z/wind/surface/level/overlay=mean_sea_level_pressure/orthographic=-80.46,19.23,328). The dark blue regions are the low air pressure centers. The grey regions are the high-pressure centers.

Figure 7c (top-middle). Tropical Storms Greg (left), Irwin (center), and Hurricane Hilary (right) spanning the East Pacific on July 24, 2017. Copied from Wiki “Tropical cyclones in 2017”, by the National Oceanic and Atmospheric Administration's Suomi NPP satellite. Copyright: Public domain.

Figure 7d (bottom-middle). The corresponding global view of Figure 7c at URL of

[https://earth.nullschool.net/#2017/07/24/0700Z/wind/surface/level/overlay=mean\\_sea\\_level\\_pressure/orthographic=-106.84,17.42,310](https://earth.nullschool.net/#2017/07/24/0700Z/wind/surface/level/overlay=mean_sea_level_pressure/orthographic=-106.84,17.42,310)

Figure 7e (top-right). Three tropical cyclones of the 2006 Pacific typhoon season at different stages of development. Copied from wiki “Tropical cyclone” at [https://en.wikipedia.org/wiki/Tropical\\_cyclone](https://en.wikipedia.org/wiki/Tropical_cyclone), NASA image by Jeff Schmaltz, MODIS Rapid Response Team, Goddard Space Flight Center. Copyright: Public domain.

Figure 8a showed an even more extreme weather condition on 7/22/2017, with a super large array of cyclone/low-pressure centers on the Pacific Ocean, with 5 centers at the West Pacific, and 4 centers at the East Pacific. Each center in the array was separated by  $\sim 20^\circ$  longitude on average. With the knowledge shown in Figure 5b, we can estimate that it can be reasonably fitted to a  $\text{Re}[Y(l,m)]$   $\theta\phi$ -2D contour map with  $m = 360^\circ/20^\circ = 18$ , and  $l \approx 35$ . So if we fill-in all the low mass density centers according to a  $\text{Re}[Y(35,18)]$   $\theta\phi$ -2D contour map, and if all low mass density centers in the range of  $10^\circ \sim 60^\circ$  latitude (both North and South) were strong enough so that they had all formed hurricanes (or cyclones) under the Coriolis force, then we would have seen an exaggerated extreme weather condition in which hurricanes (or cyclones) would have spread almost everywhere on Earth (as shown in Figure 8b). Let's name the exaggerated extreme weather condition in Figure 8b as the "extreme quantum weather", and name the extreme weather condition in Figure 8a (i.e., an array with  $\geq 9$  well-organized cyclones/low-pressure centers) as the "partial quantum weather". Now let's re-explain the whole thing in a very different angle:

- 1) A non-spin Earth's atmosphere can be described by NBP, or, equivalently, by  $\text{Re}[Y(l=0,m=0)]$ , or by  $\text{Re}[Y(l=1,m=(-1,0,1))]$ , or by  $\text{Re}[Y(l=2,m=(-2, \dots +2))]$ , or by  $\text{Re}[Y(l=15,m=(-15, \dots +15))]$ , or by a combination of all (or any) of these  $\text{Re}[Y(l,m)]$ . (Note: this is part of the Law of SMED, see SunQM-4s6). It produces a perfect spherical shell-shaped atmosphere without weather.
- 2) A spinning Earth's atmosphere can be described by NBP, or, equivalently, by  $\text{Re}[Y(l=1,m=(-1,0,1))]$ , with  $\text{Re}[Y(l=1,m=1)]$  standing out and  $\text{Re}[Y(l=1,m=0)]$  being suppressed a little bit. This generates the elliptical shape of the atmosphere and Hadley/Ferrel/Polar global circulation cells. Meanwhile, all other  $l(s)$  of  $\text{Re}[Y(l,m)]$  can be part of the spinning Earth atmosphere's QM description (because they don't change anything).
- 3) From 2), if we allow  $\text{Re}[Y(35,18)]$  mode to stand out, and suppress all other  $\text{Re}[Y(l,m)]$  modes (except the  $\text{Re}[Y(l=1,m=(0,1))]$  mode for forming the elliptical shape and Hadley/Ferrel/Polar cells), then we obtain the "extreme quantum weather" as shown in Figure 8b.
- 4) From 3), if we suppress a little bit less on other  $\text{Re}[Y(l,m)]$  modes, then the  $\text{Re}[Y(35,18)]$  mode becomes an imperfect "extreme quantum weather", which equals to a "partial quantum weather" as shown in Figure 8a.
- 5) From 4), if we suppress even less on other  $\text{Re}[Y(l,m)]$  modes, then the  $\text{Re}[Y(35,18)]$  mode may become even more imperfect than what is shown in Figure 8a, and it may have only three low mass density centers (each apart by  $\sim 20$  longitude degrees) left as shown in Figure 7b or Figure 7d.
- 6) From 5), if we suppress even less on other  $\text{Re}[Y(l,m)]$  modes, then the  $\text{Re}[Y(35,18)]$  mode may become even more imperfect, and it may have only one low mass density center (like the hurricane Dorian, or shown in Figure 6c).
- 7) From 6), if we don't suppress other  $\text{Re}[Y(l,m)]$  modes at all, then the  $\text{Re}[Y(35,18)]$  mode is completely submerged in a complete spectrum of  $\text{Re}[Y(l,m)]$  modes. Then we come back to 2), where a complete calm weather showed up.

In this way, we have used NBP and the negative peak of  $\text{Re}[Y(l,m)]$  wave function  $\theta\phi$ -2D contour map to explain the low air mass density center and the associated hurricane weather. The take-home message is: Earth's atmosphere has all QM state (wave) modes, if all these modes are perfectly evenly distributed, then the Earth's atmosphere showed a perfectly clam weather (or no weather). It is the quantum fluctuation (or the noisy distribution) of these QM state (wave) modes causes the local weather formation. If a single QM state (wave) mode standing-out locally, it causes an extreme weather in that area (like a hurricane, or an array of hurricanes). If a single QM state (wave) mode standing-out globally, it causes a global extreme weather (or a partial quantum weather, or even an extreme quantum weather). The next question is, with the climate change, will we see more and more "partial quantum weather"?

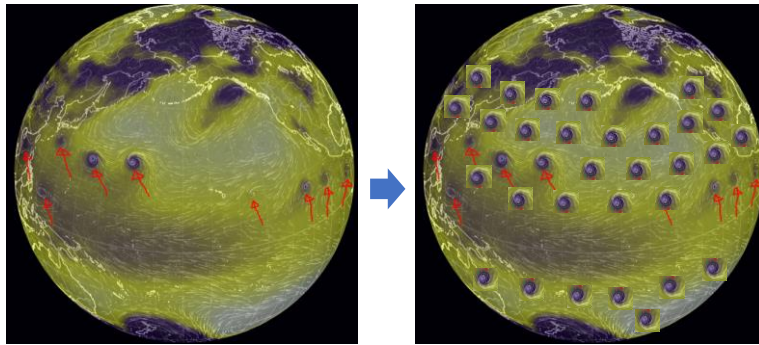


Figure 8a (left, true data). The extreme weather on 7/22/2017, at URL of [https://earth.nullschool.net/#2017/07/22/0700Z/wind/surface/level/overlay=mean\\_sea\\_level\\_pressure/orthographic=-169.54,27.87,310](https://earth.nullschool.net/#2017/07/22/0700Z/wind/surface/level/overlay=mean_sea_level_pressure/orthographic=-169.54,27.87,310)". A super large array of 9 cyclone/low-pressure centers on the Pacific Ocean.

Figure 8b (right, imagination). The exaggerated "extreme Quantum Weather". Modified based on Figure 8a by the author.

#### IV. Using NBP to analyze the extratropical cyclone

"*Extratropical cyclones ... are low-pressure areas ... in the middle latitudes of Earth between 30° and 60° latitude*" (see wiki "Extratropical cyclone"). We also can use a combined  $\text{Re}[Y(l,m)]$  wave functions to describe an extratropical (winter) cyclone. However, due to that the low air pressure center is at between 30° and 60° latitude, we can't use the Figure 6 type method (where the low-pressure center is at the "active  $\theta=90^\circ$ ") to model an extratropical cyclone, because Earth's "thermal equator" will never get to that high latitude. So we have to use the a combination of "active  $\text{Re}[Y(l,m)]$ " with the low-pressure center directly aligned at between 30° and 60° latitude. Although in theory it is doable, I (as a citizen scientist) don't have the capability to do it at this time.

#### V. Using NBP to analyze the polar vortex

Although air pressure differences (that generates the weather) can be directly generated by the air mass density differences (which directly correlates to the QM's probability density), it can also be generated by the temperature differences (which don't seem to be directly correlate to the QM's probability density). However, QM's probability density doesn't have to always correlate to mass density, it can correlate to any physical variable (as long as this physical variable generates the 1D, or 2D, or 3D wave-like variation in a QM system). For example, in the idea gas law  $VP=nRT$ , either temperature ( $T$ ), or the pressure ( $P$ ), or the air mass density ( $n$ ) can be described by QM's probability density if these variables are used to describe Earth's atmosphere (which has a  $\theta\phi$ -2D wave-like variation). In the current section, we will use QM's probability density to describe the temperature difference caused (air pressure difference generated) extreme weather.

"*A polar vortex is an upper-level low-pressure area lying near one of the Earth's poles*" (see wiki "Polar vortex"). In comparison to that a tropic (summer) cyclone is formed around a low air pressure center (caused by the low air mass density), a polar vortex is formed around a low air pressure center that is usually caused by the low temperature. According to the law of idea gas ( $PV=nRT$ ), a chunk of air, if it has an abnormally low temperature ( $T$ ) than that of surroundings, it will also have a low pressure ( $P$ ). In Earth's atmosphere, not only the air mass density distribution in  $\theta\phi$ -2D can form (or follow) the  $\text{Re}[Y(l,m)]$  wave function pattern, the air pressure or the air temperature distribution in  $\theta\phi$ -2D can also form (or follow) the  $\text{Re}[Y(l,m)]$  wave function pattern. Based on NBP, linearly combined  $\text{Re}[Y(l,m)]$  wave functions (which forms NBP) can form any kind of weather pattern: it can be air mass density-based NBP, or pressure-based NBP, or temperature-based NBP, etc. Therefore, we should be able to use NBP and a combined  $\text{Re}[Y(l,m)]$  to describe polar vortex.

Figure 9a showed a map of Earth surface air pressure at the North Pole region using the data collected on 3/24/2020. We can see that a low-pressure center (dark blue) at the North Pole is surrounded by three high pressure centers (in grey, centered around 40°N to 60°N latitude). Notice that due to the Coriolis force, at the Northern hemisphere, the air flows into the low air pressure center forming the anticlockwise swirl, and air flows out of the high air pressure center forming the clockwise swirl. That how many swirls formed at around the Polar Jet stream tells us the  $m$  quantum number of  $|nlm\rangle$  QM state. So these three high pressure centers can be (roughly) described by a  $\text{Re}[Y(l=5, m=3)]$  wave function (see Figure 9b for detailed explanation). Meanwhile, Figure 9c showed that there were five low pressure centers (in dark blue, centered around 60°S latitude) surrounding a high-pressure center at the South Pole on the same day. These five low pressure centers can be (roughly) described by a  $\text{Re}[Y(l=9, m=5)]$  wave function (see Figure 9d). So Earth poles' surface air pressure on 3/24/2020 can be (roughly) described by a NBP, or a combination of a numbers of  $\text{Re}[Y(l, m)]$  wave functions, including a  $\text{Re}[Y(5, 3)]$  wave function for the North Pole region and a  $\text{Re}[Y(9, 5)]$  wave function for the South Pole region. Notice that at even lower resolution, the South Pole's five low pressure centers can also be roughly treated as three low pressure centers, so that a  $\text{Re}[Y(5, 3)]$  wave function can describe both North and South Poles at the very low resolution.

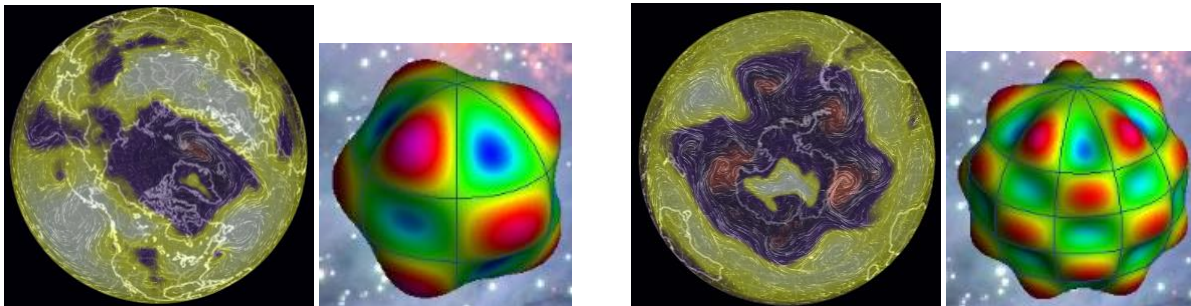


Figure 9a (left). North Pole region surface pressure map (in top-down view) on 3/24/2020. Copied from:

[https://earth.nullschool.net/#2020/03/24/0700Z/wind/surface/level/overlay=mean\\_sea\\_level\\_pressure/orthographic=-100.21,91.44,199](https://earth.nullschool.net/#2020/03/24/0700Z/wind/surface/level/overlay=mean_sea_level_pressure/orthographic=-100.21,91.44,199)

Figure 9b (middle-left), Surface (or solid) spherical harmonics plot of  $\text{Re}[Y(l=5, m=3)]$ , in side-view. The red (and the protruding) parts represent Earth's high surface pressure areas, and blue (and the recessed) parts represent Earth's low surface pressure areas.  $m=3$  was chosen to fit the three high-pressure centers in Figure 9a, and  $l=5$  was chosen to fit these high-pressure centers spanned from  $\sim 60^\circ\text{N}$  to  $\sim 25^\circ\text{N}$  latitude. Figure was generated by using the (free) online plotter at "<http://icgem.gfz-potsdam.de/vis3d/tutorial>".

Figure 9c (middle-right). South Pole region surface pressure map (in bottom-up view) on 3/24/2020. Copied from:

[https://earth.nullschool.net/#2020/03/24/0700Z/wind/surface/level/overlay=mean\\_sea\\_level\\_pressure/orthographic=-95.99,-87.21,199](https://earth.nullschool.net/#2020/03/24/0700Z/wind/surface/level/overlay=mean_sea_level_pressure/orthographic=-95.99,-87.21,199)

Figure 9d (right). Surface spherical harmonics plot of  $\text{Re}[Y(l=9, m=5)]$ , in side view.  $m=5$  was chosen to fit the five low-pressure centers in the Figure 9c, and  $l=9$  was chosen to fit these low-pressure centers spanned from  $\sim 80^\circ\text{S}$  to  $\sim 50^\circ\text{S}$  latitude.

## VI. Using NBP to analyze the meandering polar jet stream "Rossby waves" that is in standing wave mode

In an article published on the journal of "Scientific American", Michael E. Mann proposed an explanation for the extreme weather on 7/22/2018 by using quantum physics waveguide concept <sup>[19]</sup>: "The jet stream drives weather across the Northern Hemisphere. When it bends, it can create strong pressure centers that deliver high heat or heavy rain. Very large bends can get stuck in place, prolonging the extreme conditions for many days, especially during summer. Curiously, the planetary-scale physics resembles that of quantum mechanics at the atom scale. ... Pressure Centers Grow: In summer, pronounced bends in the jet stream create low-pressure systems that bring cool, wet weather and high-pressure system that produce hot, dry conditions. Sometimes the jet stream takes on a repeating, undulating pattern, following the shape of Rossby

waves created in the atmosphere as the earth rotates through it. The pattern, and weather, proceeds west to east. ... Storm Resonate: Large Rossby waves, and the jet stream bends that track them, can get stuck in place, forming a standing wave. The atmosphere can then act as a waveguide, which encourages the bands to resonate and amplify, reaching even farther north and south. The weather systems become intense and get locked in place for days. ... Destructive Day: A resonating jet stream, stalled during late July and early August 2018, touched off or magnified extreme weather around the planet. On July 22, heat waves and droughts gripped several regions and aggravated wildfires, while heavy flooding occurred in other areas". Below, using the NBP and  $\text{Re}[Y(l,m)]$  wave function  $\theta\phi$ -2D map analysis, we try to support Mann's explanation:

- 1) In Figure 11a, we chose  $\text{Re}[Y(l=13,m=7)]$  as the initial base wave function for the analysis. The low-pressure centers near the North Pole (caused by the low air temperature, see the blue dots in Figure 11a) forms a well-defined low temperature region. The interface between the cold region ( $> 60^\circ\text{N}$ , the Polar Cell) and warm region (at  $< 60^\circ\text{N}$ , the Ferrel cell) becomes a waveguide for the Polar Jet stream (see the black band in Figure 11a). We choose  $l=13$  because it makes the Polar Jet at  $\sim 60^\circ$  latitude. We choose  $m=7$  because it will generate 7 waves of Rossby wave as shown in Mann's explanation (see Figure 10). Notice that at this time the  $\text{Re}[Y(13,7)]$  wave function is on a global scale, meaning at a fixed longitude, if  $> 60^\circ\text{N}$  region is a low pressure (or low temperature, or blue) spot, then  $40^\circ\text{N} \sim 60^\circ\text{N}$  region must be a high pressure (or high temperature, or red) spot. This single  $\text{Re}[Y(13,7)]$  wave function mode on the global scale is only an over simplified model, it never really happened (or if it had happened, it would have become an "extreme quantum weather").
- 2) Usually those low pressure and low temperature centers in  $> 60^\circ\text{N}$  region are very strong, so that they forced high-pressure centers at  $< 60^\circ\text{N}$  region to re-distribute by shifting a (half-wave) phase in  $\phi$ -dimension. Then the high-pressure centers (at  $< 60^\circ\text{N}$ ) are now in between the two ( $> 60^\circ\text{N}$ ) low-pressure centers. This bends the interface (as a waveguide) between the cold region (at  $> 60^\circ\text{N}$ ) and warm region (at  $< 60^\circ\text{N}$ ), therefore caused the meandering of the polar jet stream as shown in Figure 11b. Notice that in Figure 11b,  $\text{Re}[Y(13,7)]$  mode is localized within  $> 60^\circ\text{N}$  region (or the whole Earth is no longer in a single  $\text{Re}[Y(13,7)]$  mode).
- 3) In (northern hemisphere's) winter, the ( $> 60^\circ\text{N}$ ) low-pressure centers can sometimes expand to near  $40^\circ\text{N}$ , forcing  $40^\circ\text{N} \sim 60^\circ\text{N}$  region's atmosphere to join (or to resonate with)  $> 60^\circ\text{N}$  region's  $\text{Re}[Y(13,7)]$  wave function pattern. This forms a new wave function  $\text{Re}[Y(9,7)]$ , and then this single mode dominates (or resonating) the whole region above  $40^\circ\text{N}$  latitude (as shown in Figure 11c and Figure 11d). This resonance amplified the  $\theta$ -dimensional amplitude of the jet stream 1D wave. Note: after read the wiki "Arctic Oscillation", I believe that this is more or less equivalent to the negative phase of the Arctic Oscillation.
- 4) The meandering jet stream Rossby waves (as a whole) usually rotating eastward. But at the peak of the single mode resonance, the rotational pattern may stall for a few days, causing the whole jet stream Rossby wave in a standing wave mode (see Figure 11d). Notice that Mann<sup>[19]</sup> had first used 1D well QM to describe this phenomenon in his article.

In above analysis, the driving force for the large-(latitude)-spanning resonance comes from the North Pole region's super strong low-pressure (or low-temperature) centers that intruded southward (in the northern winter). It was inspired by the data in Figure 9c, or by the data that the South Pole always has super strong, well organized low-pressure (or low-temperature) centers (see <https://earth.nullschool.net>). The North Pole region lacks of this kind of well-organized pattern because the (Pacific and Atlantic) oceans are interrupted by continents (in  $< 80^\circ\text{N}$  and  $> 40^\circ\text{N}$  latitude region). In the northern summer, the similar large-(latitude)-spanning resonance (in  $40^\circ\text{N} \sim 70^\circ\text{N}$  region) may be driven by the warm regions as mentioned in Mann's explanation.

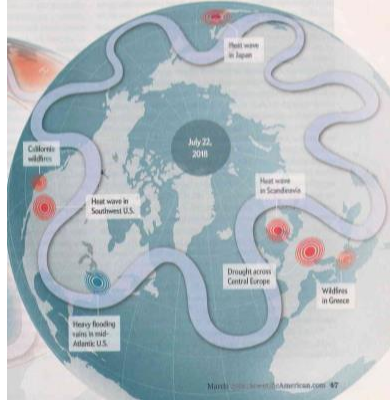


Figure 10. Copied from Mann's article <sup>[19]</sup>, to illustrate that "A resonating jet stream, stalled ... on July 22, heat waves and droughts gripped several regions and aggravated wildfires, while heavy flooding occurred in other areas". Copy permission: granted by the original author.

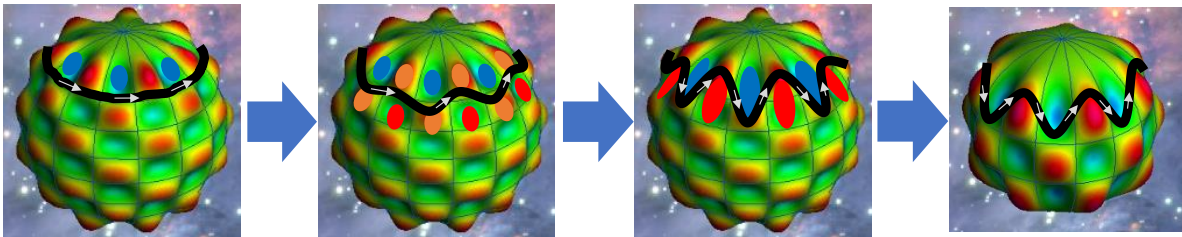


Figure 11a (left). Illustration of a polar jet stream at  $\sim 60^\circ\text{N}$  latitude (in black) based on the globalized  $\text{Re}[Y(13,7)]$  wave function map.

Figure 11b (middle-left). A relative strong but localized low-pressure centers (see blue spots in  $> 60^\circ\text{N}$  region) of  $\text{Re}[Y(13,7)]$  wave function re-distributed the high-pressure centers at  $< 60^\circ\text{N}$  region, and caused a meandering Polar Jet stream at  $\sim 60^\circ\text{N}$ . The orange spots are the low-pressure area relative to the red spots, and also the high-pressure area relative to the blue spots.

Figure 11c (middle-right). A super strong  $\text{Re}[Y(l,m=7)]$  wave function's low-pressure centers pattern (originated from  $> 60^\circ\text{N}$  region) forced  $40^\circ\text{N} \sim 60^\circ\text{N}$  region to merge with it, and formed a new  $\text{Re}[Y(l=9,m=7)]$  wave function's pattern which expanded to  $\sim 30^\circ\text{N}$  area.

Figure 11d (right). A new  $\text{Re}[Y(9,7)]$  wave function, with the jet stream Rossby wave spans from  $\sim 70^\circ\text{N}$  to  $\sim 30^\circ\text{N}$  latitude.

## VII. El Nino can also be explained by NBP in a combined $\text{Re}[Y(l,m)]$ , or by the 1D well QM

NBP can describe not only Earth's atmospheric related  $\theta\phi$ -2D phenomenon, but also Earth's ocean related  $\theta\phi$ -2D phenomenon. For example, the El Nino phenomenon. As wiki "El Niño" mentioned, "El Niño is the warm phase of the El Niño–Southern Oscillation (ENSO) ... The ENSO is the cycle of warm and cold sea surface temperature (SST)" at the equator spanning the whole Pacific Ocean between Southeast Asia ( $\sim 150^\circ\text{E}$ ) and South America ( $\sim 90^\circ\text{W}$ ), or about  $120^\circ/360^\circ$  of Earth's circumference. According to Figure 12, here we simplify the model as in two QM states, one in the normal years (including the La Nina years) in which the west Pacific has the warm water pool (near the equator), and another one in El Nino years in which the warm water pool moves to the east Pacific (also near the equator). Based on the method that used in Figure 6, we can use a combination of three  $\text{Re}[Y(l,m)]$  wave functions to model out this two QM states oscillation pattern (of course in a low resolution, as shown in Figure 13). First, we used  $\text{Re}[Y(l=3,m=3)]$  as the initial base mode. This is because in  $\theta$ -dimension,  $\text{Re}[Y(3,3)]$  wave peaks at the equator ( $\theta=\pi/2$ ), and in  $\phi$ -dimension, a single wave of  $\text{Re}[Y(3,3)]$  spans  $120/360$  of Earth's circumference (see Figure 13b, and we can adjust one wave to be in the region between  $150^\circ\text{E}$  and  $90^\circ\text{W}$  longitude to correlate to Pacific ocean's globe position). Then we added two (neighboring) wave functions  $\text{Re}[Y(2,2)]$

(see Figure 13a) and  $\text{Re}[Y(4,4)]$  (see Figure 13c) to suppress the unwanted  $\phi$ -dimensional waves beyond the  $120/360$  of Earth's circumference (by aligning the wanted wave's middle-node to the  $\phi=90^\circ$  (shown in yellow) position in the figures). Then we obtained an enhanced  $\theta\phi$ -2D wave: its  $\theta$ -dimensional wave always peaked at the equator, and it has a single  $\phi$ -dimensional (enhanced) wave with the wavelength =  $120/360$  of Earth's circumference (as shown in Figure 13d and Figure 13e). The positive amplitude of the wave (in red) represents the warm temperature region (at the west Pacific), and the negative amplitude of the wave (in blue) represents the low temperature region (at the east Pacific). So Figure 13d (2D plot) or Figure 13e (3D plot) represents the NBP  $\theta\phi$ -2D map in the normal years, while Figure 13f (3D plot) represents the NBP  $\theta\phi$ -2D map in the El Nino years. In this way, we have used NBP in a combined  $\text{Re}[Y(l,m)]$  to model out two QM states, one for the normal years, and another one for the El Nino years.

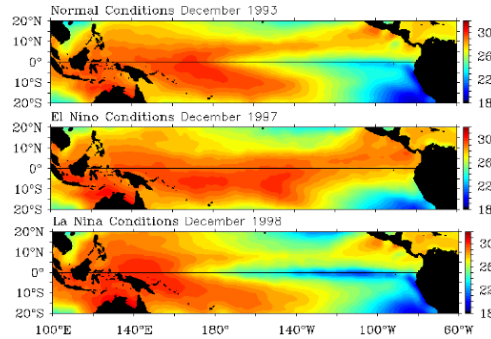


Figure 12. Pacific Ocean Temperatures during the normal condition, El Nino condition and La Nina condition. Copied from the Pacific Marine Environmental Laboratory | El Niño Theme Page, [oar.pmel.taogroup@noaa.gov](mailto:oar.pmel.taogroup@noaa.gov) at "<https://www.pmel.noaa.gov/elnino/la-nina-pacific>". Graphics are provided by the TAO project and created by Dai McClurg. Copyright: unknown.

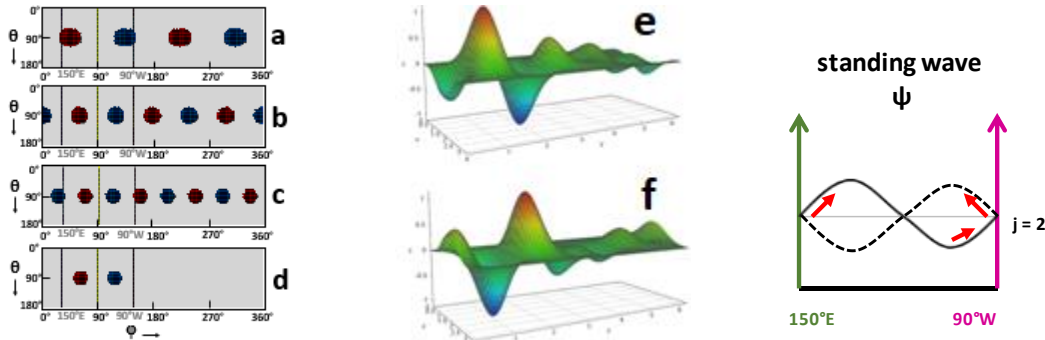


Figure 13 (a, b, c, and d, left, from top to down).  $\theta\phi$ -2D plot of  $\text{Re}[Y(2,2)]$ ,  $\text{Re}[Y(3,3)]$ ,  $\text{Re}[Y(4,4)]$ , and  $\text{Re}[Y(2,2)] + [Y(3,3)] + [Y(4,4)]/3$ , red contour  $> 0.3$ , blue contour  $< -0.3$ .

Figure 13e (middle-top).  $\theta\phi$ -3D plot of the averaged  $\text{Re}[Y(2,2)] + \text{Re}[Y(3,3)] + \text{Re}[Y(4,4)]$ , corresponding to Figure 13d.

Using "3D Surface Plotter - An online tool to create 3D plots of surfaces" at: <https://academo.org/demos/3d-surface-plotter/>

Figure 13f (middle-bottom).  $\theta\phi$ -3D plot of averaged  $\text{Re}[Y(2,2)] + \text{Re}[Y(3,3)] + \text{Re}[Y(4,4)]$  in negative.

Figure 13g (right). Illustration of a  $j=2$  standing wave in a 1D infinite deep potential well QM.

We also can use 1D square infinite deep potential well QM ( $1D\infty QM$ ) to describe the El Nino-Southern Oscillation. The 1D is the Pacific Ocean in  $\phi$ -dimension near equator, and the two continents on each side of the Pacific act as the wall of this infinity deep potential well. A standing wave (composed of a pair of warm-cold water pools) in the well with the quantum number  $j=2$  (see Figure 13f), and with two QM states: the solid line represents the normal years with the positive amplitude (= warm water pool) at the left (or Western Pacific, equivalent to Figure 13e), and the dashed line represents the El Nino years with the positive amplitude at the right (or Eastern Pacific, equivalent to Figure 13f). The dynamics of this standing wave showed that these two QM states are intensified alternatively through oscillation.

This analysis suggested that the similar oscillation of warm and cold water pools could also happen at the equator in Atlantic Ocean and India Ocean, but may be much weaker so that they are completely covered by the noisy background. The reason why the El Niño–Southern Oscillation is so strong may be because that its 1D QM well spans exactly  $1/3$  of Earth's circumference, a perfect base-tone for a spherical-surface-wave to resonate and amplify. If this is correct, then in the Pangaea era, the El Niño–Southern Oscillation could be even stronger because its 1D QM well spans exactly  $1/2$  of Earth's circumference, and  $1/2$  is even more base than that of  $1/3$  for a spherical-surface-wave's base-tone. Note: In Figure 12, if we choose La Nina vs. El Nino (instead of the normal vs. El Nino) conditions as the two QM states, then its  $\varphi$ -dimensional wavelength may should be modeled with  $1/2$  of Earth's circumference. Readers can figure out how to describe it with NBP in a combined  $\text{Re}[Y(l,m)]$  by yourself.

## Summary and Conclusion

- 1) In this paper, we tried to use NBP to describe Earth atmosphere's phenomenon in  $\theta\varphi$ -2D dimension. In section I, after analyzing Earth atmosphere's global circulation pattern, we found that it is related only to the  $\theta$ -1D QM. From the previous study (see SunQM-4s1 section V), we know that an orbital moving planet's  $\theta$ -dimensional matter wave is in a true standing wave mode, and this is also true for a spinning Earth's  $\theta$ -dimensional matter wave. Therefore, we only need to use Born probability for the analysis (because its conjugated-squaring calculation cancels out all  $\varphi$ -dimensional function, and automatically degenerated a  $\theta\varphi$ -2D QM into a  $\theta$ -1D QM). Our result in Figure 2 showed that for a true standing wave QM, Born probability analysis gives more sharp and conclusive result than the NBP analysis.
- 2) To use  $\{N,n\}$  QM's probability to describe Earth's local weather, we need to use NBP because it includes both  $\theta$  and  $\varphi$  2D information. To calculate the NBP from the known  $\text{Re}[Y(l,m)]$  wave functions, we need to first combine these  $\theta\varphi$ -2D  $\text{Re}[Y(l,m)]$  wave functions, then to subtract the  $\theta\varphi$ -2D baseline from the combined  $\theta\varphi$ -2D  $\text{Re}[Y(l,m)]$  wave functions, and then normalize the maximum to =1. However, in most cases, the  $\theta\varphi$ -2D baseline is more complicated than a straight plane (see SunQM-4s1's eq-30), hence this calculation is beyond our capability. In SunQM-4s1's Figure 10, we showed that for 1D QM, its NBP function is directly correlated to its wave function. This is still true for the  $\theta\varphi$ -2D QM. Therefore, from section II to section VII of this paper, for all  $\theta\varphi$ -2D NBP analysis, we directly use the (combined)  $\theta\varphi$ -2D  $\text{Re}[Y(l,m)]$  wave function to represent  $\theta\varphi$ -2D NBP (because NBP is directly correlate to the wave function).
- 3) Earth atmosphere's fundamental (or the low-level) structures are determined by its  $\theta$ -1D QM: its elliptical shape is caused by that the  $|2,1,1\rangle$  QM state is the most heavily populated (by air mass); its Hadley/Ferrel/Polar global circulation cells are formed by the  $|2,1,1\rangle$  QM's mass-peaking effect at  $0^\circ$  latitude and  $|2,1,0\rangle$  QM's mass-peaking effect at  $60^\circ$  latitude; and its jet streams may be explained as the residue  $|3,2,1\rangle$  and  $|3,2,0\rangle$  states embedded in the highly suppressed  $|2,0,0\rangle$  sub-shell.
- 4) Earth atmosphere's fine (or the high-level) structures are determined by its  $\theta\varphi$ -2D QM: A hurricane's low air pressure center can be described by a NBP density minimum center (or a negative peak of a combined  $\text{Re}[Y(l,m)]$  wave functions); An hurricane array can be described by that a single mode of  $\text{Re}[Y(l,m)]$  wave function is (unevenly) intensified; The polar vortex's low air pressure center can be described by a NBP density minimum center (or a negative peak of a combined  $\text{Re}[Y(l,m)]$  wave functions) of low temperature; A single day (7/22/2018)'s extreme weather can be described by a single mode of  $\text{Re}[Y(l=9,m=7)]$  wave function is (unevenly) intensified; El Nino related warm/cold water pools oscillation can also be explained by NBP in a combined  $\text{Re}[Y(l,m)]$ , or by the 1D well QM.
- 5) The result of NBP in SunQM-4 series papers clearly revealed the true physical meaning of the QM's wave function: it is the probability density of a physical variable's value, although in the wave form. This physical variable can be, for example, any one of the four physical parameters (either pressure  $P$ , or volume  $V$ , or mass density  $n$ , or temperature  $T$ ) in the idea gas law formula  $PV=nRT$ . Then, the physical meaning of the Schrodinger equation becomes: it directly describes the dynamic distribution of a physical variable's value (although in its probability's wave form), and this physical variable must belong to a QM system.

## References

- [1] Yi Cao, SunQM-1: Quantum mechanics of the Solar system in a  $\{N,n\}$  QM structure. <http://vixra.org/pdf/1805.0102v2.pdf> (original submitted on 2018-05-03)
- [2] Yi Cao, SunQM-1s1: The dynamics of the quantum collapse (and quantum expansion) of Solar QM  $\{N,n\}$  structure. <http://vixra.org/pdf/1805.0117v1.pdf> (submitted on 2018-05-04)
- [3] Yi Cao, SunQM-1s2: Comparing to other star-planet systems, our Solar system has a nearly perfect  $\{N,n\}$  QM structure. <http://vixra.org/pdf/1805.0118v1.pdf> (submitted on 2018-05-04)
- [4] Yi Cao, SunQM-1s3: Applying  $\{N,n\}$  QM structure analysis to planets using exterior and interior  $\{N,n\}$  QM. <http://vixra.org/pdf/1805.0123v1.pdf> (submitted on 2018-05-06)
- [5] Yi Cao, SunQM-2: Expanding QM from micro-world to macro-world: general Planck constant, H-C unit, H-quasi-constant, and the meaning of QM. <http://vixra.org/pdf/1805.0141v1.pdf> (submitted on 2018-05-07)
- [6] Yi Cao, SunQM-3: Solving Schrodinger equation for Solar quantum mechanics  $\{N,n\}$  structure. <http://vixra.org/pdf/1805.0160v1.pdf> (submitted on 2018-05-06)
- [7] Yi Cao, SunQM-3s1: Using 1st order spin-perturbation to solve Schrodinger equation for nLL effect and pre-Sun ball's disk-lyzation. <http://vixra.org/pdf/1805.0078v1.pdf> (submitted on 2018-05-02)
- [8] Yi Cao, SunQM-3s2: Using  $\{N,n\}$  QM model to calculate out the snapshot pictures of a gradually disk-lyzing pre-Sun ball. <http://vixra.org/pdf/1804.0491v1.pdf> (submitted on 2018-04-30)
- [9] Yi Cao, SunQM-3s3: Using QM calculation to explain the atmosphere band pattern on Jupiter (and Earth, Saturn, Sun)'s surface. <http://vixra.org/pdf/1805.0040v1.pdf> (submitted on 2018-05-01)
- [10] Yi Cao, SunQM-3s6: Predict mass density r-distribution for Earth and other rocky planets based on  $\{N,n\}$  QM probability distribution. <http://vixra.org/pdf/1808.0639v1.pdf> (submitted on 2018-08-29)
- [11] Yi Cao, SunQM-3s7: Predict mass density r-distribution for gas/ice planets, and the superposition of  $\{N,n\}$  or  $|\ln m\rangle$  QM states for planet/star. <http://vixra.org/pdf/1812.0302v2.pdf> (submitted on 2019-03-08)
- [12] Yi Cao, SunQM-3s8: Using  $\{N,n\}$  QM to study Sun's internal structure, convective zone formation, planetary differentiation and temperature r-distribution. <http://vixra.org/pdf/1808.0637v1.pdf> (submitted on 2018-08-29)
- [13] Yi Cao, SunQM-3s9: Using  $\{N,n\}$  QM to explain the sunspot drift, the continental drift, and Sun's and Earth's magnetic dynamo. <http://vixra.org/pdf/1812.0318v2.pdf> (submitted on 2019-01-10)
- [14] Yi Cao, SunQM-3s4: Using  $\{N,n\}$  QM structure and multiplier  $n'$  to analyze Saturn's (and other planets') ring structure. <http://vixra.org/pdf/1903.0211v1.pdf> (submitted on 2019-03-11)
- [15] Yi Cao, SunQM-3s10: Using  $\{N,n\}$  QM's Eigen  $n$  to constitute Asteroid/Kuiper belts, and Solar  $\{N=1..4,n\}$  region's mass density r-distribution and evolution. <http://vixra.org/pdf/1909.0267v1.pdf> (submitted on 2019-09-12)

[16] Yi Cao, SunQM-3s11: Using  $\{N,n\}$  QM's probability density 3D map to build a complete Solar system with time-dependent orbital movement. <http://vixra.org/pdf/1912.0212v1.pdf> (original submitted on 2019-12-11)

[17] Yi Cao, SunQM-4: Using full-QM deduction and  $\{N,n\}$  QM's non-Born probability density 3D map to build a complete Solar system with orbital movement. <http://vixra.org/pdf/2003.0556v1.pdf> (submitted on 2020-03-25)

[18] Yi Cao, SunQM-4s1: Is Born probability merely a special case of (the more generalized) non-Born probability (NBP)? <http://vixra.org/pdf/2005.0093v1.pdf> (submitted on 2020-05-07)

[19] Michael E. Mann. The weather amplifier, strange waves in the jet stream foretell a future full of heat waves and flood, Scientific American, Mar.2019, pp43.

[20] Wiki "Atmosphere of Earth" figure "*Comparison of the 1962 US Standard Atmosphere graph of geometric altitude against air density, pressure, the speed of sound and temperature with approximate altitudes of various objects*". Author: Cmglee.

[21] A series of my papers that to be published (together with current paper):  
 SunQM-4s2: Using  $\{N,n\}$  QM and non-Born probability to analyze Earth atmosphere's global pattern and the local weather.  
 SunQM-4s3: Schrodinger equation and  $\{N,n\}$  QM.  
 SunQM-4s4: More explanations on non-Born probability (NBP)'s positive precession in  $\{N,n\}$  QM.  
 SunQM-4s6: "Simultaneous-Multi-Eigen-Description (SMED)" is one of many nature attributes of  $\{N,n/q\}$  QM ...  
 SunQM-4s7: Addendums, Updates and Q/A for SunQM series papers.  
 SunQM-5: A new version of QM based on interior  $\{N,n\}$ , multiplier  $n'$ ,  $|R(n,l)|^2 * |Y(l,m)|^2$  guided mass occupancy, and RF, and its application from string to universe (drafted in April 2018).  
 SunQM-5s1: White dwarf, neutron star, and black hole re-analyzed by using the internal  $\{N,n\}$  QM (drafted in April 2018).

[22] Major QM books, data sources, software I used for this study:

Douglas C. Giancoli, Physics for Scientists & Engineers with Modern Physics, 4th ed. 2009.

David J. Griffiths, Introduction to Quantum Mechanics, 2nd ed., 2015.

John S. Townsend, A Modern Approach to Quantum Mechanics, 2nd ed., 2012.

Stephen T. Thornton & Andrew Rex, Modern Physics for scientists and engineers, 3rd ed. 2006.

James Binney & David Skinner, The Physics of Quantum Mechanics, 1st ed. 2014.

Wikipedia at: <https://en.wikipedia.org/wiki/>

(Free) online math calculation software: WolframAlpha (<https://www.wolframalpha.com/>)

(Free) online spherical 3D plot software: MathStudio (<http://mathstud.io/>)

(Free) offline math calculation software: R

(Free) online "Earth: a global map of wind, weather and ocean" at "<https://earth.nullschool.net>".

(Free) online Surface spherical harmonics plotter at "<http://icgem.gfz-potsdam.de/vis3d/tutorial>".

Microsoft Excel, Power Point, Word.

Public TV's space science related programs: PBS-NOVA, BBC-documentary, National Geographic-documentary, etc.

Journal: Scientific American.

**Note: I hope to get all my SunQM series papers posted at arXiv.org. If you are a qualified arXiv-endorser and willing to endorse anyone of my 19 papers, please let me know. Thank you very much for your help.**